International Journal of
Molecular Sciences

MDPI

Article

4-Methylumbeliferone Treatment at a Dose of 1.2 g/kg/Day Is Safe for Long-Term Usage in Rats

Kateřina Štěpánková [1,2], Dana Mareková [1,2], Kristýna Kubášová [3], Radek Sedláček [3], Karolína Turnovcová [1], Irena Vacková [1,4], Šárka Kubinová [1,5], Pavol Makovický [6], Michaela Petrovičová [1], Jessica C. F. Kwok [1,7,*,†], Pavla Jendelová [1,2,†] and Lucia Machová Urdzíková [1,2,*,†]

1 Institute of Experimental Medicine, Czech Academy of Sciences, 14220 Prague, Czech Republic
2 Department of Neuroscience, Second Faculty of Medicine, Charles University, 15006 Prague, Czech Republic
3 Department of Mechanics, Biomechanics and Mechatronics, Faculty of Mechanical Engineering, Czech Technical University in Prague, 16000 Prague, Czech Republic
4 Institute of Physiology, Czech Academy of Sciences, 14220 Prague, Czech Republic
5 Institute of Physics, Czech Academy of Sciences, 18221 Prague, Czech Republic
6 Department of Biology, Faculty of Education, J. Seyle University, SK-94501 Komarno, Slovakia
7 School of Biomedical Sciences, Faculty of Biological Sciences, University of Leeds, Leeds LS2 9JT, UK
* Correspondence: j.kwok@leeds.ac.uk (J.C.F.K.); lucia.machova@iem.cas.cz (L.M.U.)
† These authors contributed equally to this work.

Abstract: 4-methylumbelliferone (4MU) has been suggested as a potential therapeutic agent for a wide range of neurological diseases. The current study aimed to evaluate the physiological changes and potential side effects after 10 weeks of 4MU treatment at a dose of 1.2 g/kg/day in healthy rats, and after 2 months of a wash-out period. Our findings revealed downregulation of hyaluronan (HA) and chondroitin sulphate proteoglycans throughout the body, significantly increased bile acids in blood samples in weeks 4 and 7 of the 4MU treatment, as well as increased blood sugars and proteins a few weeks after 4MU administration, and significantly increased interleukins IL10, IL12p70 and IFN gamma after 10 weeks of 4MU treatment. These effects, however, were reversed and no significant difference was observed between control treated and 4MU-treated animals after a 9-week wash-out period.

Keywords: hyaluronan; 4-methylumbelliferone; chondroitin sulphates; neuroplasticity

Citation: Štěpánková, K.; Mareková, D.; Kubášová, K.; Sedláček, R.; Turnovcová, K.; Vacková, I.; Kubinová, Š.; Makovický, P.; Petrovičová, M.; Kwok, J.C.F.; et al. 4-Methylumbeliferone Treatment at a Dose of 1.2 g/kg/Day Is Safe for Long-Term Usage in Rats. *Int. J. Mol. Sci.* **2023**, *24*, 3799. https://doi.org/10.3390/ijms24043799

Academic Editors: Joanne Tipper and Javad Tavakoli

Received: 23 December 2022
Revised: 6 February 2023
Accepted: 9 February 2023
Published: 14 February 2023

1. Introduction

4-methylumbeliferone (4MU) is used in several European countries under the name 'hymecromone' as a treatment for biliary disorders, based on its choleretic and biliary anti-spasmodic activity. The hepatocellular formation of bile is dependent on the active secretion of bile salts (i.e., bile-dependent pathway) and the active transport of sodium ions across the canalicular membrane (bile-independent pathway), which represents a luminal meshwork of tubules between adjacent hepatocytes [1]. This site is important for primary bile formation [2]. It has been suggested that the choleretic activity of 4MU is mediated by the active transport of sodium ions into the bile capillaries and thus enhances the bile flow, which is not dependent on the osmotic force of bile acids [3]. 4MU rapidly decreases the concentration of bicarbonate and chloride ions in bile and thus increases the cation anion gap in the bile duct. The mechanism is believed to be dependent on the conversion of 4MU to the 4-methylumbelliferyl glucuronide in the liver. 4-methylumbelliferyl glucuronide presented in its anionic form is then coupled with sodium ions and actively secreted to the biliary tree, and water passively follows [3]. In addition to its choleretic activity, 4MU is also an inhibitor of hyaluronan (HA) synthesis [4], and HA has been shown to be a potential cure for a number of diseases through the inhibition of HA synthesis, ranging from reducing cancer metastasis in oncologic conditions through ischaemia reperfusion injury to

non-alcoholic steatohepatitis. An overview of 4MU doses, 4MU administration time and experimentally treated diseases is summarised in the Supplementary Materials (Table S1).

Recently, it has been proposed that 4MU may serve as a novel plasticity treatment for central nervous system conditions through perineuronal net (PNN) modulation [5–8]. PNNs are extracellular matrix (ECM) structures that primarily surround brain inhibitory parvalbumin interneurons and spinal motoneurons. These structures stabilise the established neuronal connections and thus limit the plasticity in the matured CNS [9] by restricting plastic changes from environmental adaptation [10]. HA and chondroitin sulphates (CSs) are key components of the PNNs and they share one common monosaccharide residue, glucuronic acid. The binding of 4MU to glucuronic acid reduces the production of UDP-glucuronic acid for HA synthesis [11]. We have previously shown that oral treatment of 4MU reduces PNNs and thus increases the neuroplasticity after spinal cord injury [6] and enhances memory [5]. Besides the experimental application, there are several clinical trials using 4MU. The treated conditions, doses and the current status of the trials are given in the Supplementary Materials (Table S2).

Due to its property of reducing perineuronal nets, 4MU appears to be a drug with potential for many CNS pathologies such as CNS trauma, memory disorders and neurodegenerative diseases [5,6,12,13]. The pharmacokinetics of 4MU in human and rats have been reported when trials were performed for cholestasis [14,15]. However, long-term administration of 4MU at 1.2 g/kg/day, such as that used in spinal cord injury treatment, could potentially develop adverse side effects. It is therefore important to access the effect of long-term 4MU treatment in other organs.

The objectives of this pharmacology study were to identify the possible adverse pharmacological properties of 4-MU that could be relevant for future long-term application in spinal cord injury models.

The current study characterises the effects mediated by the long-term application (10 weeks) of orally administered 4MU at a dose of 1.2 g/kg/day on CNS, liver, spleen, heart, small intestine, bone marrow and blood. We also studied the biomechanical changes in tendons and skin due to the prevalence of HA and CSPGs in these tissues. Finally, the effect of a 2-month long wash-out period was also examined. The results demonstrate that long-term 4MU administration induces minimal adverse effects in organs and does not lead to any irreversible effects. During the 10-week treatment, we observed decreased levels of HA and CSPGs, significantly increased bile acids corresponding with the 4MU-mediated choleretic activity, as well as increased blood sugars and proteins a few weeks after 4MU administration. Significantly increased interleukins IL10, IL12p70 and IFN gamma after 10 weeks of 4MU treatment were also observed. However, no significant differences were found between control-treated and 4MU-treated animals after the 9-week wash-out period.

2. Results

2.1. 1.2 g/kg/Day Dose of 4MU Downregulates HA throughout the Body

Hyaluronan is not only a major polysaccharide component of the extracellular matrix, but also plays a key role in the regulation of many cellular processes and in the organisation of tissue architecture [16]. Our previous results have suggested that 4MU can be considered as a potential treatment for CNS pathologies [6,8]. Here, we investigated the potential adverse effects induced by long-term systemic administration of 4MU at a dose of 1.2 g/kg/day. Immunohistochemical analysis of HABP and ACAN or CS-56 were performed in brain, spinal cord, spleen, liver and kidney (Figures 1 and 2). We observed significant downregulations of staining intensity in the tissues, confirming the effect of 4MU in HA and CS reduction.

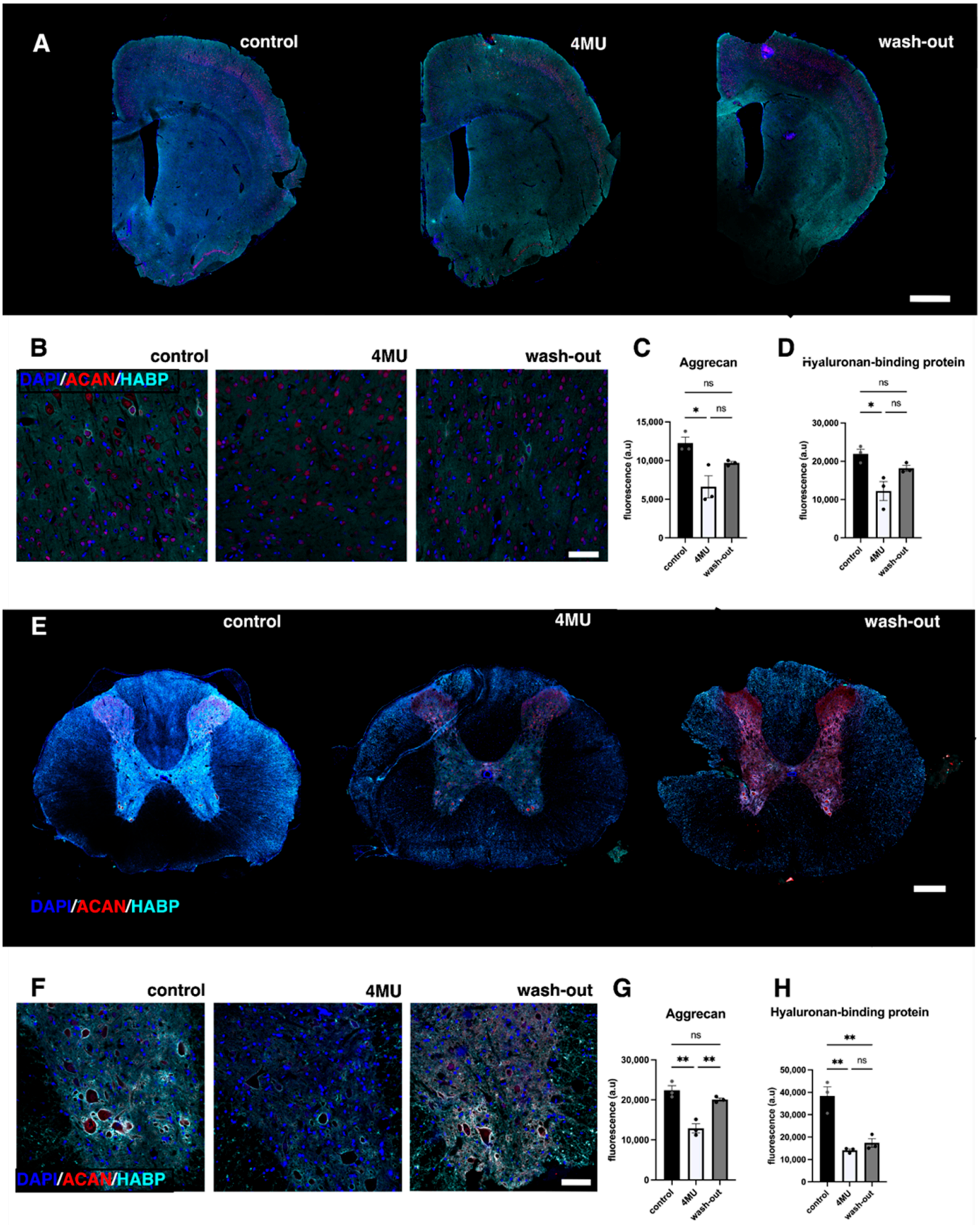

Figure 1. 4MU administered at a dose of 1.2 g/kg/day downregulates HA as well as PNNs in brain and spinal cord after 10 weeks of administration. (**A**) Representative confocal images showing HA-

and ACAN-positive areas in brain sections in placebo-fed animals, 4MU-treated animals and animals after 9 weeks of wash-out period. Scale bar: 1000 µm. (**B**) Representative confocal images showing detail of the brain cortex. In 4MU-treated animals, HA and ACAN positivity is reduced compared to untreated controls and partially returns after the 9 week wash-out period. Scale bar: 50 µm. (**C**,**D**) Quantification of ACAN (red) and HABP signal in the brain cortex. The values are the means ± SEM for $n = 3$ in each group. (**E**) Representative confocal images showing HA (turquoise)-, ACAN (red)- and DAPI (blue)-positive areas in spinal cord sections in placebo-fed animals, 4MU-treated animals and animals after 9 weeks of wash-out. Scale bar: 200 µm. (**F**) Representative confocal images showing detail of the spinal ventral horns. In 4MU-treated animals, HA and ACAN positivity is reduced compared to untreated controls and partially returns after 9 weeks of wash-out, as observed in the brain. Scale bar: 50 µm. (**G**,**H**) Quantification of ACAN- and HABP-positive signals in spinal grey matter. The values are the means ± SEM; * $p < 0.05$, ** $p < 0.01$ by one-way ANOVA with Tukey's multiple comparisons test, $n = 3$ in each group. ns: no significance.

4-MU treatment in healthy animals decreased the intensity of both ACAN- and HABP-positive signals in the brain by almost 50% (ACAN: 46.16 ± 6.23%, $n = 3$; $p = 0.0128$; HABP: 44.26 ± 5.71%, $n = 3$, $p = 0.0141$; Figure 1A–H). After 9 weeks of wash-out period, the intensity did not return to more than 83% (ACAN: 79.1 ± 2.02%, $n = 3$; $p = 0.1287$; HABP: 72.9 ± 4.07%, $n = 3$, $p = 0.0956$; Figure 1A–D). In the spinal cord, there was an even stronger decrease in the fluorescent signal after 4-MU treatment (ACAN: 42.35 ± 4.62%, $n = 3$; $p = 0.0012$; HABP: 63.26 ± 4.07%, $n = 3$, $p = 0.00015$; Figure 1E–H). After 9 weeks of wash-out, the level of aggrecan signal returned to almost 90% (ACAN: 89.7 ± 2.08%, $n = 3$; $p = 0.2911$). In contrast to the ACAN-positive signal, the HA level in the spinal cord returned to the original values (HABP: 45.29 ± 11.19%, $n = 3$, $p = 0.9932$; Figure 1E–H). Aggrecan was chosen as one of the markers of PNNs. In order to stain for CSPGs in other organs, we decided to replace aggrecan with CS-56 for visualisation in kidney, spleen and liver sections. 4-MU treatment demonstrates different effect in organs in healthy animals. In the liver, our results indicate a significantly reduced CS-56-positive signal (25.56 ± 1.13%, $n = 3$; $p = 0.0173$, Figure 2A,D,E), but the HABP-positive signal had no significant difference even after 4-MU treatment.

In the spleen, we did not observe any significant changes between any of the three groups (Figure 2B,D,E). In the kidney, we observed an increase in the fluorescence intensity of CS-56 (31.23 ± 7.64%, $n = 3$; $p = 0.0018$), and a decrease in HABP fluorescence intensity (44.88 ± 4.08%, $n = 3$, $p = 0016$; Figure 2C–E). Following 9 weeks of wash-out period, the CS-56-positive signal in the liver remained low compared to healthy controls ($p = 0.0009$), in contrast to the kidney samples, where the CS-56-postive signal remained high after the wash-out period ($p = 0.0247$).

2.2. Neither Haematological nor Biochemical Parameters Indicate Adverse effects Caused by Long-Term Administration of 4MU at the Same Dose

We then investigated whether long-term treatment with 1.2 g/kg/day 4MU affects any of the haematological parameters, including leukocytes, haemoglobin, haematocrit, erythrocytes (concentration, mean volume and colorant), red cell distribution width, thrombocytes, reticulocytes, neutrophils, lymphocytes, monocytes, eosinophils, basophils and neutrophils (Figure 3). The data are presented in Supplementary Materials, Table S2. Haematological parameters from all three groups were compared with reference values ("Clinical Laboratory Parameters for Crl:Wi (Han) rats", Charles River Laboratories International, 2008). All parameters were within the reference range, except for absolute and relative monocyte counts, where data fell outside the reference range. In the case of monocytes, the numbers increased in all three groups without any significant difference.

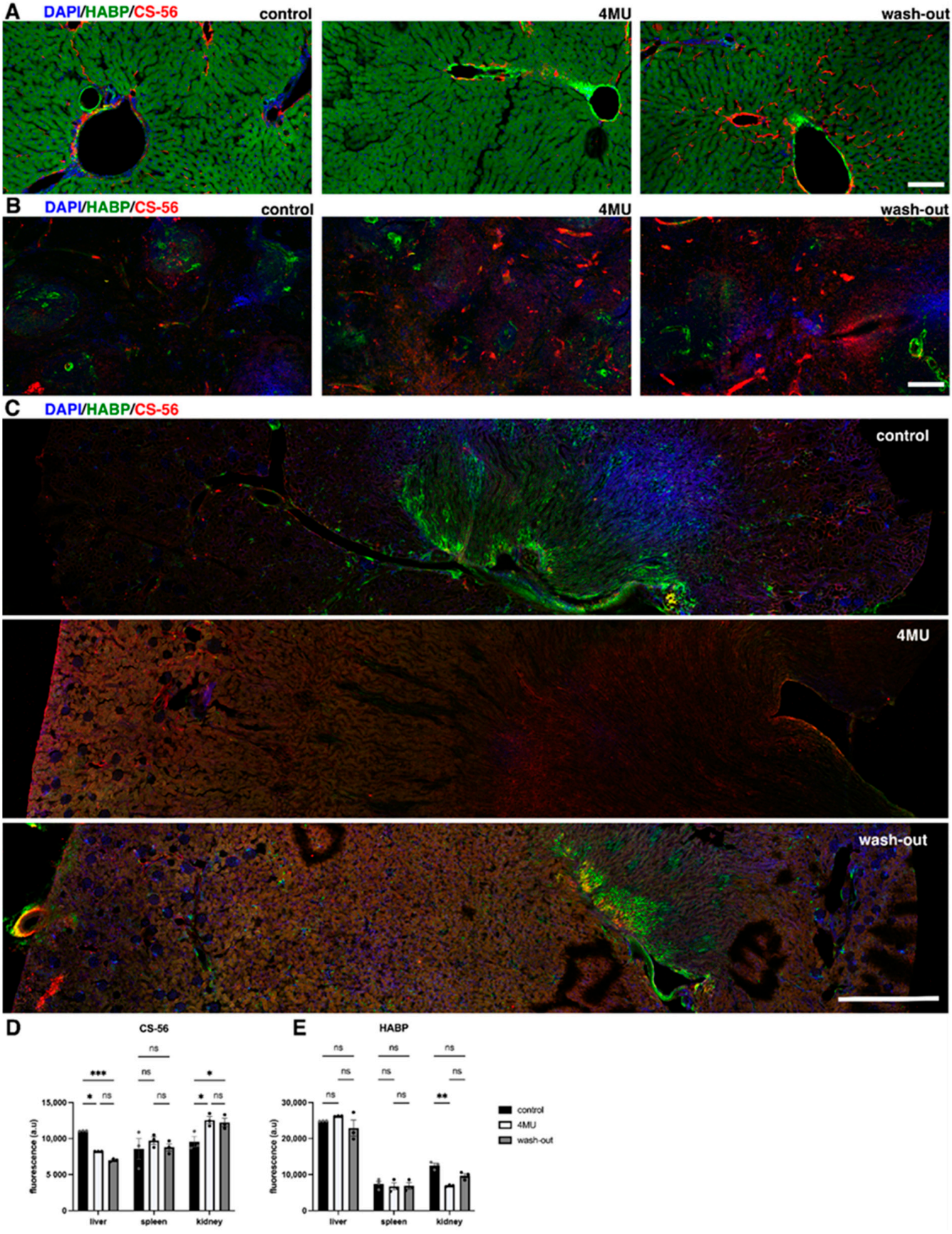

Figure 2. 4MU administered at a dose of 1.2 g/kg/day leads to downregulation of HA and CSPGs throughout the body. (**A**) Representative confocal images showing HA- and CSPG-positive areas in

(**A**) liver, scale bar 100 µm, (**B**) spleen, scale bar 200 µm, and (**C**) kidney, scale bar 1000 µm, in placebo-fed animals, 4MU-treated animals and animals after 9 weeks of wash-out, indicating downregulation of both markers and the return of signal after 9 weeks of wash-out. (**D**,**E**) Quantification of CS-56- and HABP-positive signals in the kidney, spleen and liver sections. The values are the means ± SEM, * $p < 0.05$, ** $p < 0.01$, *** $p < 0.001$ by two-way ANOVA with Tukey's multiple comparisons test, $n = 3$ in each group. ns: no significance.

Next, we tested the biochemical parameters of blood and blood serum. The following parameters were monitored: sodium, potassium, calcium, phosphorus, creatinine, urea (Table S3) and markers associated with liver injury (total bilirubin, bile acids, AST, ALT, ALP) (Figure 3). Since almost all drug classes can cause a drug-induced liver injury [17], we focused primarily on liver function tests to monitor potential liver injury. In week 7 of 4MU treatment, we observed significant differences in the measured ALT level between the wash-out group (1.189 ± 0.080 µkat/L) and placebo (0.886 ± 0.097 µkat/L). Moreover, we observed slightly higher ALT enzyme levels (mean 1.005 ± 0.133 µkat/L) than the reported reference value (0.3–0.75 µkat/L) throughout the experiment.

4MU has been shown to increase bile acid secretion and is used in biliary stasis [18]. We thus checked the concentration of bile acid after 4MU treatment. We observed a significantly higher level of bile acids in the blood at 4 weeks post treatment when compared to control (4MU 79.36 ± 29.67 µmol/L, wash-out 96.36 ± 28.69 µmol/L vs. control 14.15 ± 3.11 µmol/L; $p = 0.0014$ and $p < 0.0001$, respectively). In week 7, the bile acid level remains high in the treated group, although significance is only observed in the wash-out group, reflecting a potential physiological adaptation to 4MU from long-term treatment (4MU 46.07 µmol/L, wash-out 71.37 ± 10.78 µmol/L vs. 21.296 ± 12.803 µmol/L; $p = 0.38$ and $p = 0.0235$, respectively). Our data revealed no other significant differences between the groups in the remaining haematological markers of liver injury.

The results suggest that long-term 4MU treatment did not induce any serious adverse changes in haematological or biochemical parameters in blood.

The levels of serum glucose, cholesterol, triacyl glycerides and iron were also evaluated in blood serum. The data are presented in Supplementary Materials, Table S4. No renal impairment was observed after 10 weeks of treatment with 4MU at a dose of 1.2 g/kg/day.

Based on the histochemical changes in the kidneys, glucose and protein levels were analysed every three weeks (Table S4). Glycosuria, an abnormal amount of glucose present in the urine, is usually associated with impaired kidney filtration. Glycosuria was observed in the fourth week in the 4MU-treated group (0.443 ± 0.167 g/L) and in the wash-out group (0.424 ± 0.155 g/L) compared to the placebo group (0.032 ± 0.011 g/L) (Figure 4A). In weeks 7 and 10, the urinary glucose results remained slightly increased in the 4MU-treated and wash-out groups compared to the reference values, but there was no significant difference from the placebo group. During the wash-out period, urine glucose levels returned to the normal physiological range (Figure 4A).

Kidney damage is often associated with elevated urinary protein levels, referred to as proteinuria. Proteins outside normal physiological values were observed in the 4MU-treated and wash-out groups (Figure 4B), as well as in the placebo group in week 1 (0.179 ± 0.064 g/L) and week 10 (0.179 ± 0.038 g/L) of the sampling period. Only in week 7, there was a significant difference in the placebo group (0.103 ± 0.030 g/L) compared to the 4MU-treated (0.271 ± 0.057 g/L) and wash-out (0.313 ± 0.052 g/L) groups. During the wash-out period, protein levels did not return to physiologically normal values (Figure 4B).

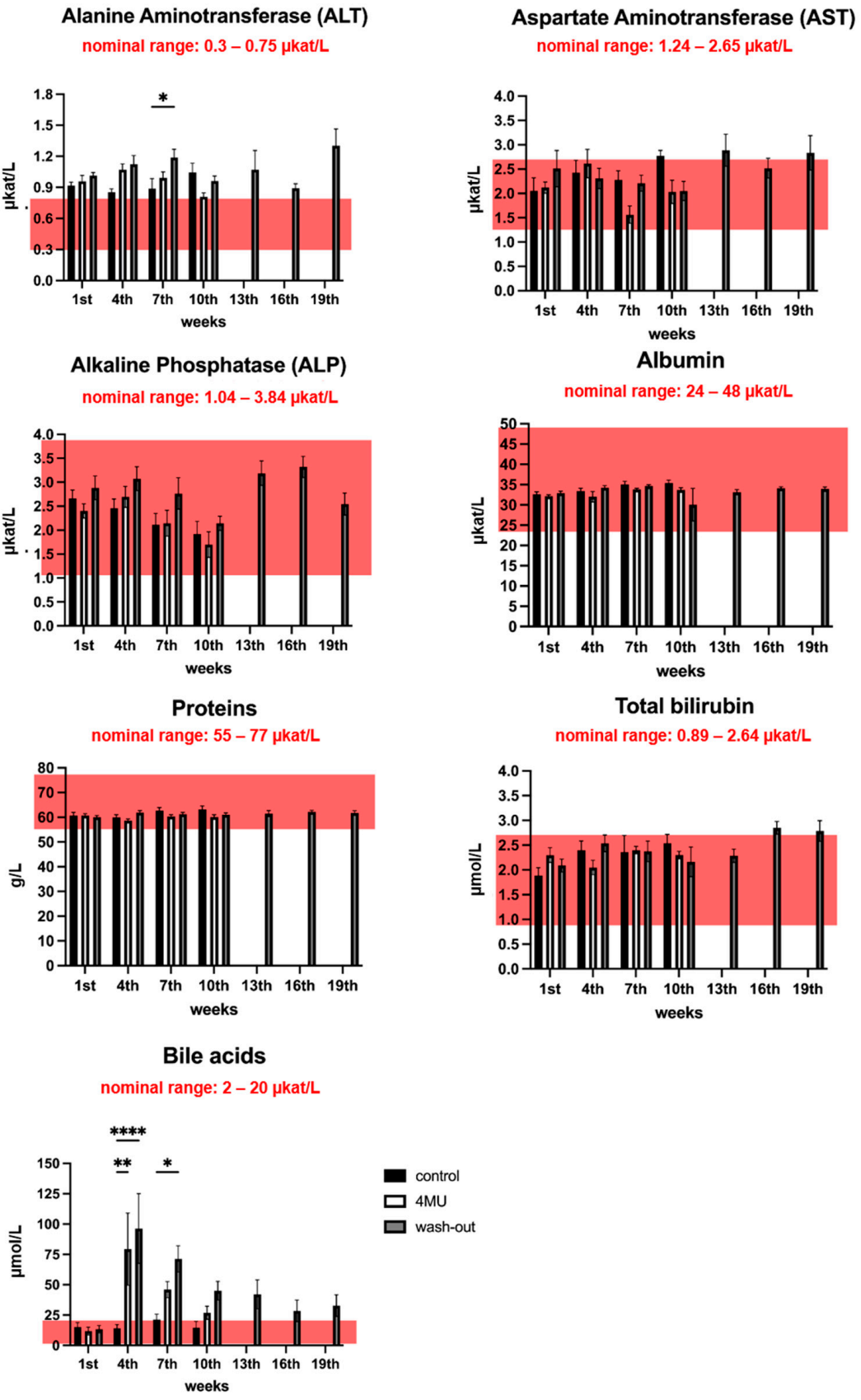

Figure 3. Liver function tests do not indicate any liver damage after long-term 4MU treatment at 1.2 g/kg/day dose. The pink box in each graph indicates the nominal range of the corresponding test. * $p < 0.05$, ** $p < 0.01$, **** $p < 0.0001$ by two-way *ANOVA* with Tukey's multiple comparisons test, $n = 5$ to 7.

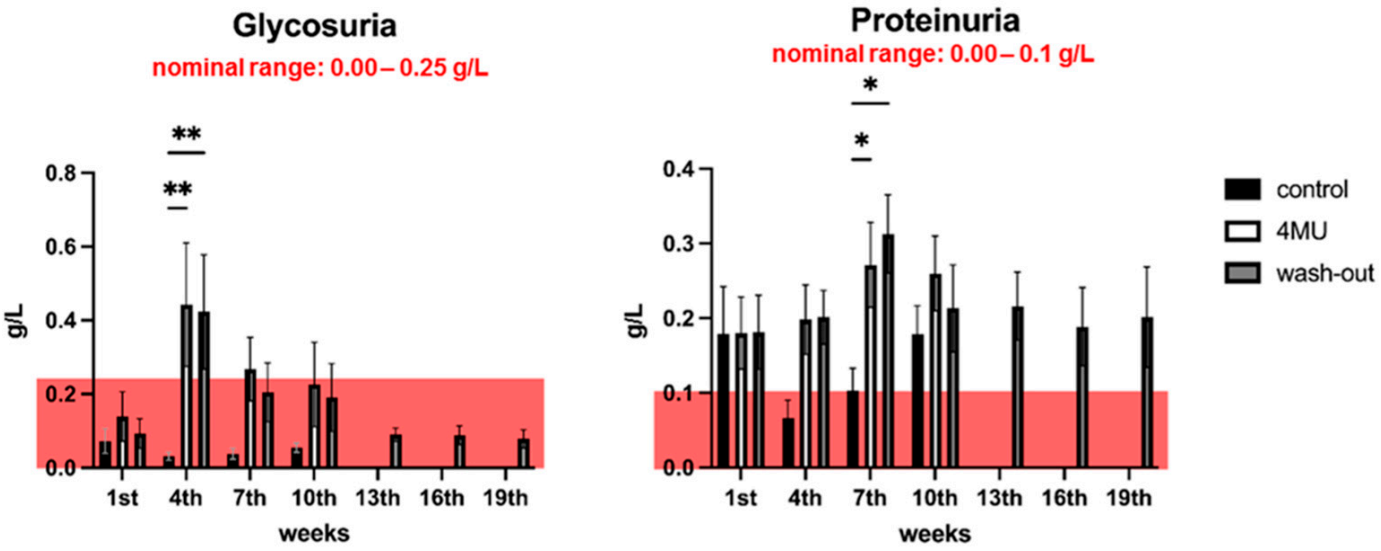

Figure 4. Glycosuria and proteinuria show no severe kidney damage after 1.2 g/kg/day of 4MU-treatment. The bar graph shows the level of urinary glucose changes (**A**) and urinary protein changes (**B**) during the 4MU treatment. The pink box in each graph indicates the nominal range of the corresponding test. Data are expressed as a mean ± SEM; * $p < 0.05$, ** $p < 0.01$ by two-way *ANOVA* with Tukey's multiple comparisons test, $n = 7$.

To further investigate the effect of drug metabolism on renal injury, the Rat Kidney Toxicity 5-Plex ProcartaPlex Panel 2 (Invitrogen, #EPX050-30125-901) was used. Five urinary biomarkers were chosen to assess nephrotoxicity (Figure 5): clusterin, cystatin C (Cys-C), neutrophil gelatinase-associated lipocalin (NGAL), urinary tissue inhibitor of metalloproteinases-1 (TIMP-1) and albumin. Clusterin is usually associated with tubulointerstitial renal lesions, and drug-induced damage is manifested by reduced gene and protein expression. Cys-C is filtered, completely reabsorbed and catabolised in the proximal tubule under physiological conditions. In acute kidney injury, the urinary concentration of Cys-C increases. NGAL, an iron-transporting protein, increases its urinary excretion after nephrotoxic and ischemic insults, and thus is among the biomarkers of acute kidney injury [19]. TIMP-1 levels are low in healthy kidneys, but have been shown to increase significantly in models of kidney diseases and are also associated with the extent of fibrosis [20]. The last marker studied was albumin, a well-established diagnostic and prognostic marker for assessing the degree of glomerular disease severity in the progression of chronic kidney disease. Our results showed significantly reduced levels of clusterin in the wash-out group (12.861 ± 1442 pg/mL) compared to the placebo (19.903 ± 2121 pg/mL) and the 4MU-treated group (18.115 ± 647 pg/mL). No significant differences were observed between groups in Cys-C, NGAL, TIMP-1 and albumin levels.

2.3. 1.2 g/kg/Day Dose of 4MU Increases Levels of IFN-γ, IL10 and IL12p70 in Blood Serum after 10 Weeks of Daily Administration but Values Returned Back to Control Levels during the Wash-Out Period

As there is evidence showing that HA regulates cytokine release [7], we investigated whether 4MU-mediated inhibition of HA synthesis would affect the process. The Complete 14-Plex Rat ProcartaPlex™ Panel (Invitrogen, #EPX140-30120-901) was used to measure the concentration of fourteen cytokines (IFN-γ, IL10, IL12p70, IL13, IL2, IL17a, IL4, IL5, IL6, IL1α, IL1β, TNF-α, GM-CSF and G-CSF) in blood serum. However, we were only able to detect six of them. The other eight markers were either negative or below the detection limit of the kit.

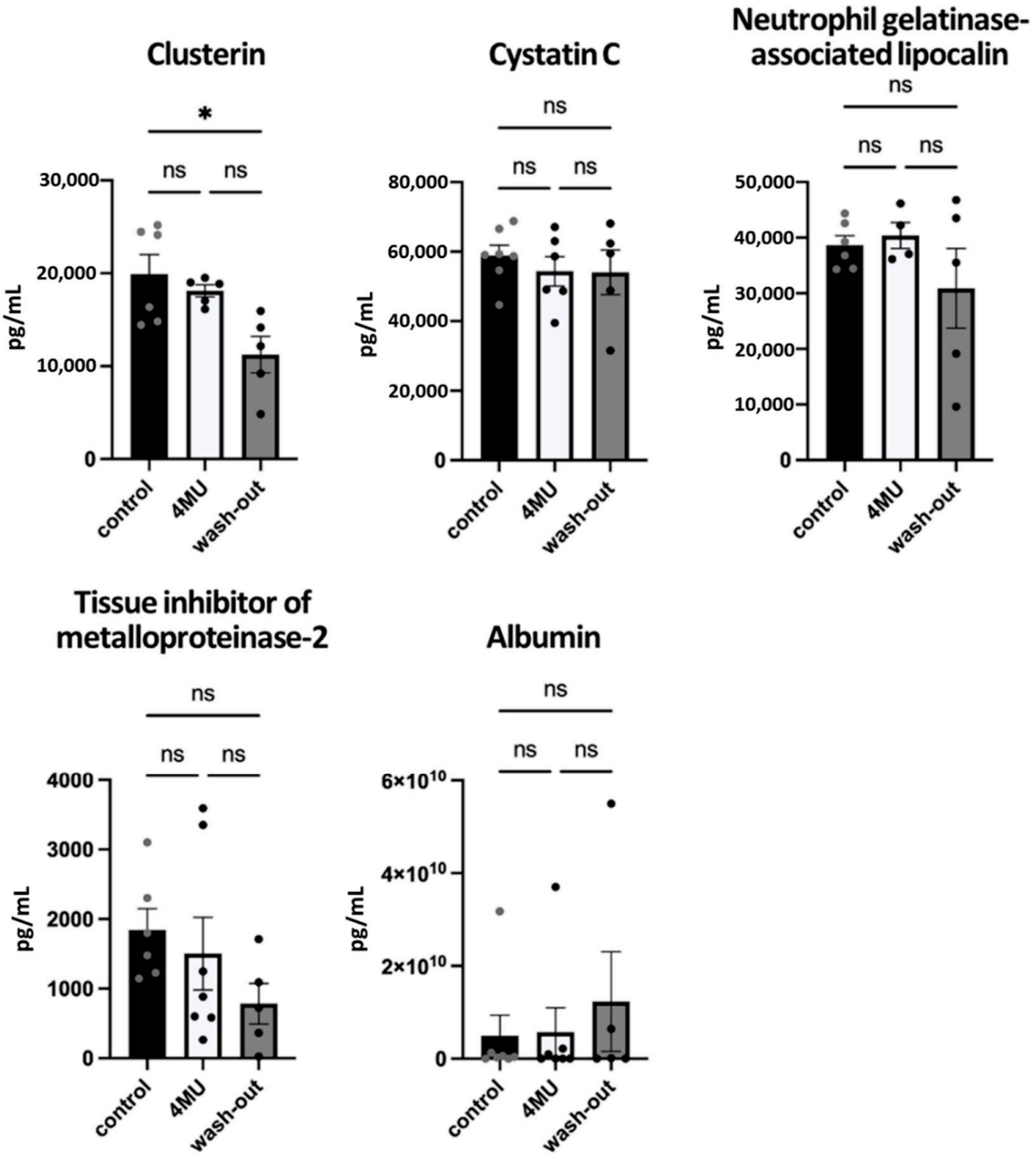

Figure 5. Urinary biomarkers used to assess the nephrotoxicity. Bar graphs show the level of urinary markers of renal injury. Data are expressed as a mean ± SEM; * $p < 0.05$ by one-way *ANOVA* with Tukey's multiple comparisons test, $n = 4$ to 7. ns: no significance.

Our results indicate significantly increased levels of IFN-γ, IL10, IL12p70, and G-CSF in 4MU-treated animals when compared to the control placebo group, with a decrease back to the control values in the wash-out group. Furthermore, after the wash-out period, the values of all markers affected by 4MU treatment returned to those of healthy controls. IL13 and IL2 were not significantly altered compared to the control group (Figure 6).

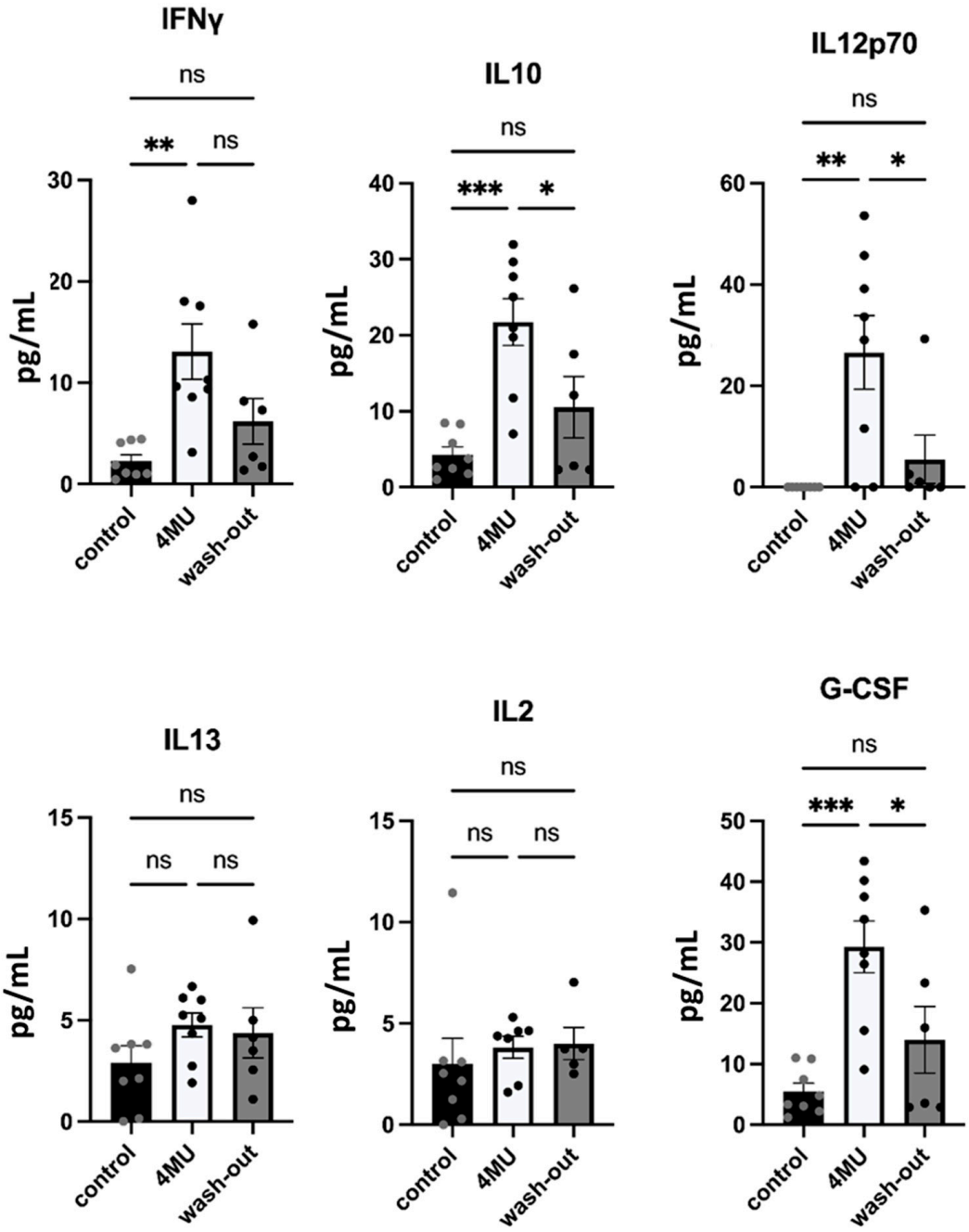

Figure 6. Serological levels of cytokines and interleukins after long-term 4MU treatment. Bar graphs show the level of detected cytokines and interleukins. Data are expressed as a mean ± SEM; * $p < 0.05$, ** $p < 0.01$, *** $p < 0.001$ by one-way ANOVA with Tukey's multiple comparisons test, $n = 5–8$. ns: no significance.

2.4. 1.2 g/kg/Day Dose of 4MU Does Not Affect Behavioural Performance of the Experimental Animals

Various behavioural tests were used to determine the possible behavioural changes that 4MU might have on locomotor functions in rats (Figure 7). Grip strength test was used to assess neuromuscular functions by determining the maximum force exhibited by the animal. Animals in the wash-out group had significantly reduced isometric forelimb contraction strength compared to the control placebo group, but the reduction was mild. Rotarod was used to assess motor function and forelimb-hindlimb coordination. No significant changes were found between groups.

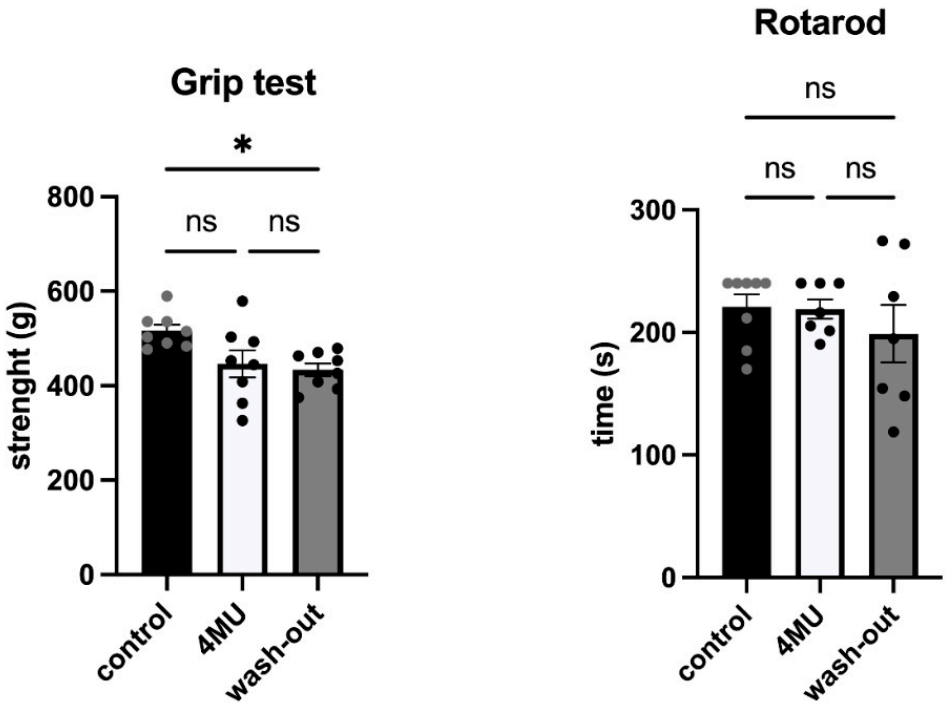

Figure 7. The results between placebo, 4MU-treated and wash-out groups did not show any changes in motor functions after 10 weeks of 4MU treatment, but significant difference was observed in the strength of the forelimbs between placebo and wash-out groups. Different color dots are used for easy identification of each data points. Data are expressed as mean ± SEM; * $p < 0.05$ by one-way *ANOVA* with Tukey's multiple comparisons test. ns: no significance.

2.5. 1.2 g/kg/Day Dose of 4MU Increases the Relative Number of Proerythroblasts in Bone Marrow, but Returned to Normal after the Wash-Out Period

HA plays a key role in the highly complex regulatory network of the hematopoietic microenvironment [21]. Accordingly, we examined bone marrow smears to assess the effect of 4MU treatment on haematopoiesis. The results showed significant changes in the percentage of proerythroblasts in the smear. Proerythroblasts, the earliest of the four developmental stages of the normoblast, were significantly higher in the 4MU-treated group compared to the placebo and wash-out groups. HA forms a regulatory element in the hematopoietic microenvironment [21], suggesting that 4MU-mediated HA inhibition disrupts this microenvironment, which is crucial for successful haemopoiesis and leads to a significant increase in the number of proerythroblasts per 1000 cells in 4MU-treated animals (Figure 8).

2.6. Long-Term 4MU Treatment at the Current Dose Does Not Affect the Biomechanical Properties of Tendons and Skin

There are several studies evaluating the contribution of HA to tendon growth and maturation [22] and skin turgor [23]. To evaluate whether 4MU-mediated HA inhibition affects skin or/and tendon integrity, biomechanical properties were measured (Table 1). The mechanical properties of rat skin were evaluated using a uniaxial tensile test. The results obtained from the mechanical tests showed no statistical differences ($p = 0.05$) between the Young's modulus of elasticity in the skin tension, determined at two values of longitudinal relative strain of 5% and 10%, for the placebo control group (Young's tensile modulus of 9.326 (7.57–10.97) MPa at 5%, and 16.43 (10.79–17.37) MPa at 10%), the 4MU-treated group (13.57 (10.45–16.47) MPa at 5%, and 16.06 (8.82–17.13) MPa at 10%) and the wash-out group (10.43 (8.43–12.27) MPa, and 16.79 (12.29–20.20) MPa at 10%).

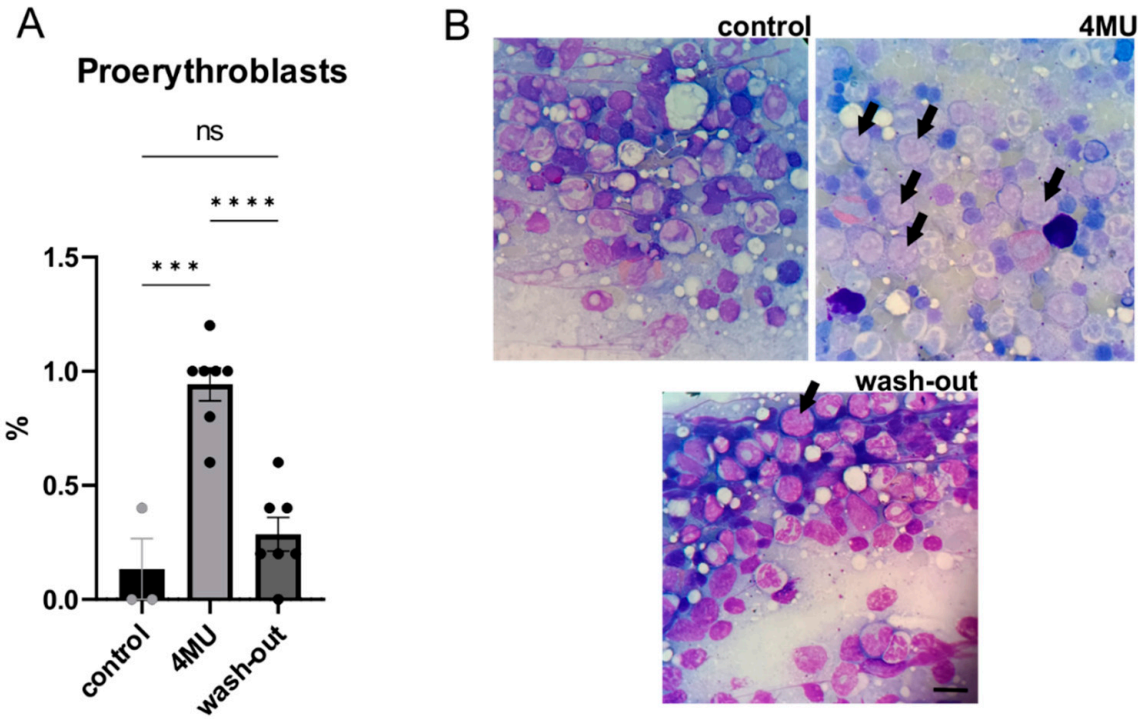

Figure 8. Relative number of proerythroblasts in the bone marrow. (**A**) shows the bar graph comparing the relative number of proerythroblasts in 1000 cells in bone marrow per the smear; (**B**) shows representative images of the bone marrow smear. Black arrows show the proerythroblasts; scale bar: 20 μm; $n = 8$; *** $p < 0.01$; **** $p < 0.001$ by one-way *ANOVA* with Tukey's multiple comparisons test. ns: no significance.

Table 1. The biomechanical properties of skin and tendon in control, 4MU and wash-out groups.

Skin		
Young modulus E5 (5%)/MPa	control	9.326 ± 1.113
	4MU	13.57 ± 1.856
	wash-out	10.43 ± 1.240
Young modulus E10 (10%)/MPa	control	16.43 ± 2.910
	4MU	16.06 ± 2.702
	wash-out	16.79 ± 3.704
Tendons		
Maximum force Fmax/N	control	20.11 ± 2.673
	4MU	14.75 ± 1.746
	wash-out	23.56 ± 3.708
Maximum stress σmax/Nm^{-2}	control	23.2 ± 3.015
	4MU	22.51 ± 3.531
	wash-out	38.83 ± 7.662

The mechanical properties of the tendons were evaluated by uniaxial tensile test. The results showed that there was no statistical difference between the tensile strength of the Achilles tendon and ultimate strength value for the placebo group, the 4MU-treated group and the wash-out group ($p = 0.05$). The ultimate strength value from the tensile test was 20.11 ± 2.673 N for the placebo control group, 14.75 ± 1.746 N for the 4MU-treated group and 23.56 ± 3.708 N for the wash-out group. The tensile strength of the Achilles tendon

reached 23.2 ± 3.015 in the placebo group, 22.51 ± 3.531 in the 4MU-treated group and 38.83 ± 7.662 in the wash-out group. The tensile strength value of the wash-out group increased by up to 178% of that of the placebo group, but this difference was not statistically significant ($p = 0.05$).

3. Discussion

In this study, we investigated the systemic effects after a 10-week 4MU treatment followed by an 8-week wash-out. The results showed that the levels of HA and CSPGs were reduced. Corresponding with the 4MU-mediated choleretic activity, there was a significant increase in bile acids. There was also an increase in blood sugars and proteins a few weeks after 4MU administration. In addition, the level of interleukins IL10, IL12p70 and IFN gamma significantly increased after 10 weeks of 4MU treatment. However, no significant differences were found between control-treated and 4MU-treated animals after the 9-week wash-out period. The results suggest that long-term 4MU treatment is well-tolerated and does not induce adverse effects on normal physiology.

4MU was previously identified as an inhibitor of HA synthesis. HA is a non-sulphated glycosaminoglycan composed of disaccharide repeats of D-glucuronic acid (GlcA) and N-acetyl-D-glucosamine. 4MU inhibits HA synthesis by depleting UDP-glucuronic acid (UDP-GlcA), which is an essential substrate for HA, via glucuronidation of 4MU [24–26]. In addition, this leads to a reduction in HAS mRNA levels [27]. Here, we report that 4MU also reduces the synthesis of CS, which shares the same monosaccharide, GlcA, as the key basic component. As CS is a key inhibitory molecule for neural regeneration and plasticity, our results suggest that 4MU could potentially be applicable for a novel non-invasive treatment for nervous system conditions.

In our experiments, we used a systemic route of administration and assumed that the whole body of the animal would be affected. In order to investigate the systemic effect of 4MU treatment at a dose of 1.2 kg/g/day, we decided to map the pathophysiological changes in more detail. Our results showed that long-term 4MU administration did not cause irreversible adverse effects.

HA is evolutionary conserved and abundantly expressed throughout the body. As a simple linear polysaccharide, HA exhibits a wide range of biological functions. HA interacts with various molecules, thereby maintaining tissue homeostasis and organising the structure of the ECM. The exceptional biophysical and biomechanical properties of HA contribute to tissue hydration, mediate the diffusion of solutes through the extracellular space and maintain tissue lubrication. Binding of HA to cell surface receptors activates numerous signalling pathways that regulate cell function, tissue development, inflammation progression, wound healing responses and tumour biology, as reviewed in [28] (Figure 9). In the CNS, HA regulates neuronal and glial cell differentiation, neuronal activity and plays a role in neurodegenerative diseases and CNS injuries (summarised in [29]). HA is also associated with the dense ECM structure that enwraps certain types of neurons in the brain and the spinal cord, called PNNs, where it forms the PNN backbone [30]. After treatment with 4MU at the current dose, we observed downregulation of HA and PNNs in the brain and spinal cord. Indeed, we have previously observed that 4MU treatment enhances memory retention in adult mice [5]. However, PNNs have recently been shown to be involved in several psychiatric disorders such as schizophrenia, autism spectrum disorders and mood disorders [31]. This suggests that pharmacological dose assessment is only the first step in evaluating the effect of 4MU, and behavioural studies addressing the potential development of psychiatric disorders following PNN downregulation will be needed for future clinical relevance.

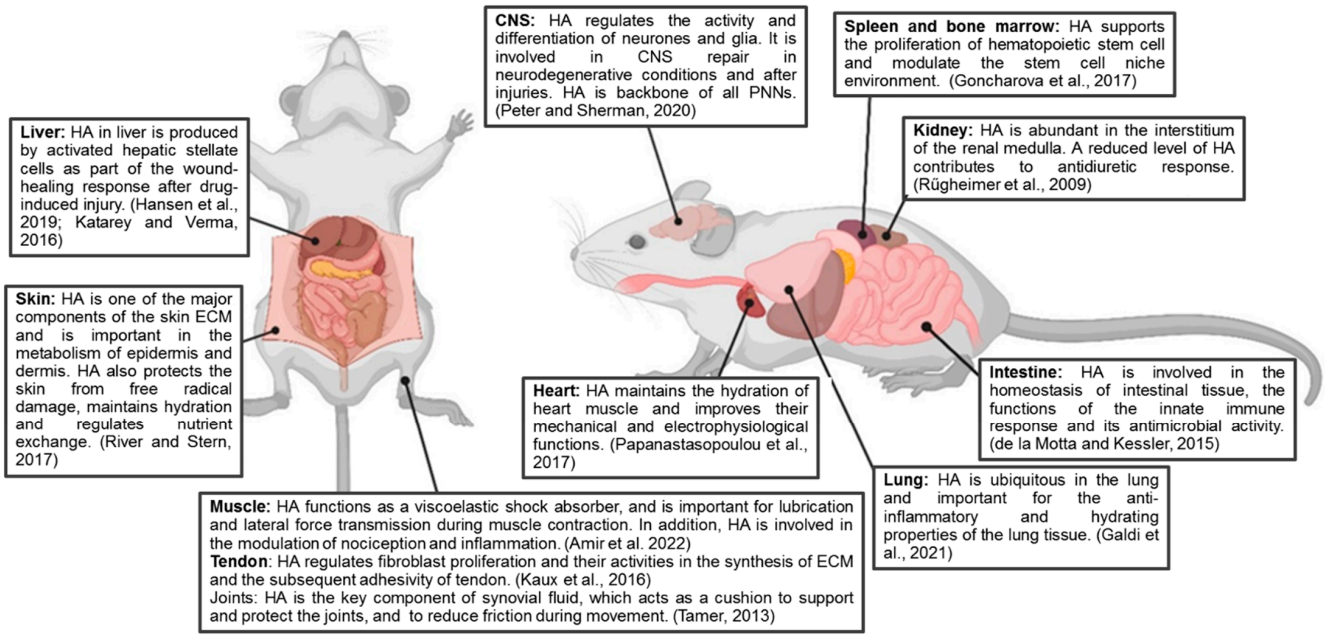

Figure 9. Schematic representation showing the diverse biological functions which HA is involved. Created with BioRender.com, Refs. [21,29,32–40].

Outside the CNS, HA also regulates the physiological functions of other organs. In the lungs, HA is mainly present in the lung connective tissue [41] and is involved in the formation of viscous gel, which plays a key role in tissue homeostasis, in the regulation of fluid balance in the lung interstitium and their biomechanical integrity [42]. We did not observe any pathological changes in histology after treatment with 4MU at the current dose, suggesting that the current dose administered for 10 months does not lead to structural changes in lung tissue.

HA is abundant in the heart, where it is involved in cardiac physiological functions [43] as well as in pathological conditions [44]. Although HA is one of the key molecules in the heart, improving electrophysiological and mechanical functions, the reduction in HA after treatment with 4MU in our study is not indicative of pathological changes in the heart tissue.

HA in the spleen is important for CD-44-mediated progenitor cell adhesion. When the affinity for CD-44 is dysregulated following impaired HA synthesis, this is accompanied by morphological changes in the spleen such as striking enlargement [45] and increased hyaluronidase activity, causing impaired GAG metabolism in the connective tissue [46]. We did not observe any significant changes in splenic HA distribution and/or any pathology between the groups in the histological examination of the spleen. On the contrary, we observed significant changes in bone marrow smear after long-term 4MU treatment. Bone marrow is composed of many cell types, such as bone-forming osteoblasts and hematopoietic stem cells. HA forms an essential element in the regulatory network of haematopoiesis. In the hematopoietic microenvironment, HA is actively involved in the regulation of cytokine and chemokine production and cell motility [47]. In our experiment, we observed a significantly high proportion of proerythroblasts in the 4MU-treated group compared with the placebo and wash-out groups. Proerythroblasts are the earliest stage cells out of the four in the development of normoblasts. Thus, they demonstrate the important role that ECM plays in haemopoiesis by allowing hematopoietic cells to adhere to the marrow stroma and also bind growth factors controlling haemopoiesis [48]. The close contact facilitated by the ECM has been shown to be a controlling factor required for successful haematopoiesis [21]. This suggests that 4MU-mediated inhibition of HA synthesis results in the loss of some of the cell–cell interactions necessary for successful haemopoiesis and leads to a significantly

higher relative number of proerythroblasts per 1000 cells in 4MU-treated rats compared with the other groups.

The liver has been shown to be the most important organ involved in the synthesis and degradation of HA [49], and at the same time, the key organ for detoxification. Glucuronidation is one of the major mechanisms for drug detoxification and requires UDP-GlcA, the key substrate for HA synthesis. 4MU administered to the body will be removed through this metabolism in the liver. To investigate the effect of 4MU on the liver itself, liver function tests were performed. We monitored two of the enzymes: ALT and AST. We observed slightly higher levels of ALT in all three groups throughout the experiment when compared to the reference range. In the seventh week, we also observed significantly increased ALT in the wash-out group compared to the placebo group. It has been shown that liver enzyme levels can change even under normal physiological conditions [50] or as a result of intense physical activity [51]. In the case of AST [52], our data showed that AST levels were within the physiological range throughout the duration of the experiment.

In addition to liver enzymes, we also examined albumin, total protein, bilirubin and bile acids in the blood throughout the experiment. Albumin and the total protein levels were within the physiological norms throughout the experiment. The last marker monitored was bilirubin, a breakdown product of red blood cells, and elevated levels may also indicate liver damage. Our biochemical results together with pathological examination revealed no liver damage after long-term 4MU treatment at the current dose, suggesting that 4MU at this dose does not lead to drug-induced damage even after 10 weeks of daily administration.

In the gut, HA facilitates nutrient and water absorption as well as the continuous interaction with GAG-rich (glycosaminoglycans) interstitial ECM [53]. During pathological conditions when nutrient and water intake are compromised, HA distribution is altered [54]. Under pathophysiological conditions where HA synthesis is disrupted, increased bacterial translocation and dysbiosis occurs, as well as permeabilisation mediated by disrupted tight junctions. In addition, there is recruitment of mononuclear cells and increased adhesion in lamina propria. We did not observe any pathophysiological changes in the intestine or other complications related to intestinal damage following long-term 4MU treatment.

Over the past decades, HA has emerged as a key player in nephrology and urology studies involving ECM organisation, inflammation, regeneration, as well as pathological processes [55]. With reference to 4MU, it has already been shown that HA inhibition could be protective against renal ischaemia reperfusion injury [56]. Despite the fact that we observed a loss of HA when staining renal sections for HABP, we did not observe any pathological changes after 10 weeks of 4MU treatment. Urinary biochemical evaluation revealed glycosuria in week 4 and proteinuria in week 7 in 4MU-treated animals. Markers of nephrotoxicity did not indicate any evidence of kidney damage. The only significant difference was observed in urinary clusterin levels. A significant reduction in clusterin levels was observed in the wash-out group compared to the placebo, which may be related to the age of the animals rather than to the 4MU treatment itself.

In mammals, about 27% of total HA is expressed in the skeleton and connective tissue, whereas only about 10% is expressed in muscle [57]. Studies have already shown that HA is mainly concentrated in joint synovial fluid, skin and muscle connective tissue [58], fascia and loose connective tissue [59]. HA plays a key role in lubrication as well as in lateral force transmission during muscle contraction [60]. To test muscle contraction and muscle strength, the animals were behaviourally tested on rotarod and grip strength. We did not observe any significant difference between the placebo and the 4MU-treated group that would indicate impairment of muscle contraction or strength. The significant difference observed between the placebo and wash-out groups in the grip strength test is likely related to age-related changes in the neuromuscular system [61]. Due to the high expression of HA in tendons, where it enhances fibroblast cellular activity [36], and in synovial fluid [37] between joints, which protects bone ends and provides support during movement, we

also tested the biomechanical properties of tendons. Our results suggested no significant changes indicating an adverse effect of 1.2 g/kg/day 4MU.

HA was found to be responsible for skin moisture in the skin [62] and wound healing [63]. HA is synthetised by both dermal but also epidermal cells. Dermal HA, unlike epidermal HA, is primarily responsible for skin hydration. A decrease in epidermal HA is directly associated with skin ageing; on the other hand, dermal HA has been shown to remain constant with ageing [64]. Our results suggest that the 4MU treatment did not lead to downregulation of HA in the skin nor alter the biomechanical properties.

HA is also an important player in the regulation of the immune response [65]. As part of the immune response, inflammation plays a key role in the body's defence against pathogens. However, inappropriate activation of inflammatory processes can contribute to many pathological conditions [66]. IFN-γ and IL10 have been described in the context of hyaluronan synthesis, and both appear to inhibit chemokine gene expression by altering mRNA stability and transcription of MIP-1α and MIP-1β genes [67]. Furthermore, IL10 plays an important role as a regulator of HA synthesis in addition to its role in anti-inflammatory responses. IL10 binds to IL10R1 and IL10R2 to form a tetrameric complex and activates the JAK/STAT3 pathway. This pathway leads to phosphorylation and nuclear translocation of STAT3, which activates genes such as hyaluronan synthase (HAS) [68]. This could explain the significantly higher IL10 levels in 4MU-treated animals as an attempt by the organism to compensate for the 4MU-mediated HA inhibition.

4. Materials and Methods

4.1. Animals

Healthy 10-week-old female Wistar rats (n = 24,250 $\pm$ 30 g) were obtained from Janvier Labs (CS 4105 Le Genest Saint Isle; Saint Berthevin Cedex 53941 France). This study involved only female rats to reduce the potential interference from rapid weight gain observed in male rats in long-term study. Animals were assigned randomly into 3 groups (n = 8/group): placebo group, treated group (4MU) and wash-out group. For the whole duration of the experiment, the rats were housed in pairs under a 12 h light/dark cycle with standard conditions. Rats received tap water and food *ad libitum*.

After 10 weeks of the 4MU treatment, animals from placebo and 4MU-treated groups were intraperitoneally anesthetised with a lethal dose of ketamine (100 mg/kg) and xylazine (20 mg/kg). Animals were then transcardially perfused with phosphate-buffer saline (PBS) and 4% paraformaldehyde in PBS. The wash-out group was sacrificed after another 9 weeks.

The experiments were approved by the ethical committee of the Institute of Experimental medicine of ASCR and performed in accordance with Law No. 77/2004 of the Czech Republic. Based on previous studies, the number of animals was statistically optimised for each particular experiment to achieve their reduction according to the European Commission Directive 2010/63/EU.

4.2. Drug Dosage

Rats were fed *ad libitum* with chocolate-flavoured chow (Sniff GmbH, Soest, Germany) (placebo) or with chocolate-flavoured pellets containing 4MU (4-methylumbelliferone, DbPharma France) at a dose of 1.2 g/kg/day $\pm$ 10% of 4MU (i.e., 2.5% w/w dose in the chow). The 10% variation represents the variability of food intake between rats, and also between individual weeks. The animals were treated for 10 weeks. The wash-out group was fed with 4MU for 10 weeks, after which they were left untreated for a further 9 weeks. Rats and chow consumed were weighed weekly throughout the 4MU treatment. While each rat was weighed individually, the chow was then weighed from the food hopper and an average of the chow consumption was calculated.

4.3. Haematology and Biochemistry

Animals were anesthetised with an inhalant mixture of isoflurane and air (3 v/v% isoflurane, AbbVie, Chicago, IL, USA), with an inflow of 300 mL/min, and kept under

anaesthesia for the entire duration of the blood sample collection. Blood was collected from the retro-orbital venous sinus by inserting an autoclaved Pasteur pipette tip into the medial canthus of the eye under the nictitating membrane. The pipette tip was positioned between the globe and the bony orbit of the eye. Blood was collected every 3 weeks (in the 1st, 4th, 7th, 10th week of the experiment in all three groups and in weeks 13, 16, 19 in the wash-out group). Blood samples were collected into BD Microtainer® blood collection tubes. Blood samples for haematological analysis were collected in anticoagulant tubes containing K2EDTA (#365974), and the following parameters were assessed: red blood cells count, haemoglobin, haematocrit, white blood cell count and relative number of white blood cells. Blood samples for biochemical analysis were collected in a serum-separating tube (#365963), and the following serum parameters were determined: sodium, potassium, calcium, phosphorus, urea, creatinine and total bilirubin. Results were evaluated by Synlab (Munich, Germany).

While the animal was still under anaesthesia, urine was collected. The rat was held over a Petri dish, and by manual pressure on the lower abdominal area, urine was squeezed out of the bladder. The urine was collected with a syringe into an Eppendorf tube (1.5 mL). In every sample, levels of glucose and proteins were assessed. Urine was evaluated by Synlab (Munich, Germany) as blood samples.

4.4. Immunohistochemistry

Brain and spinal cord tissue were embedded in O.C.T. compound (VWR) and sectioned in a frozen block of tissue into 40 µm thick slices for further immunohistological staining. At room temperature (RT), free-floating 40 µm sections were washed 3 times for 10 min each in 1x PBS in order to remove cryoprotectant (ethylene glycol:glycerol:PBS; 3:3:4) residue. Tissue was then permeabilisated with 0.5% triton in PBS for 2 h. Then, the Avidin/Biotin blocking kit (Abcam; ab64212) was used to decrease non-specific signal by blocking the endogenous biotin. Tissue was then blocked in the solution containing ChemiBLOCKER (Millipore, Darmstadt, Germany #2170; 1:10), 0.3 M glycine, 0.2% triton, PBS) for another 2 h. The sections were then transferred to co-incubate at 4 °C in immunoblockade containing the following antibodies: biotin-conjugated HABP (b-HABP; Amsbio #AMS.HKD-BC41; 1:200; 48 h); anti-ACAN (rabbit; Sigma, Darmstadt, Germany #AB1031; 1:300; 48 h); anti-CS-56 (mouse; Sigma #C8035; 1:200; 48 h). To visualise each primary antibody staining, the tissue was then co-incubated with the appropriate species of fluorescent-conjugated secondary antibodies (Invitrogen, Darmstadt, Germany, #S32354; #S21374; #A-11005; #A-11037; 1:300; 6 h; RT). Then, DAPI (4',6-diamidino-2-phenylindole, dihydrochloride) in 0.2% triton in PBS was used (Invitrogen #D1306; 1:2000; 10 min). Samples were mounted in Mowiol® mounting media. Samples were observed and captured with Zeiss LSM 880 Airyscan microscope (Carl Zeiss AG; Oberkochen, Germany) to evaluate the HA and ACAN/CSPGs changes in organ sections. Three replicate sections were imaged for all organs on a Zeiss LSM 880 confocal microscope and analysed in FIJI™ (NIH ImageJ). Image analysis parameters were kept constant among all samples.

4.5. Proteomics

For evaluation of kidney toxicity, proteins in urine were evaluated using the Kidney Toxicity 5-Plex Rat ProcartaPlex™ Panel 2 (Invitrogen # EPX050-30125-901). Prior to the transcardial perfusion, urine samples were manually collected from each rat, then stored in −80 °C. The Rat Kidney Toxicity 5-Plex ProcartaPlex Panel 2 allows the analysis of 5 protein targets, namely albumin, cystatin, clusterin (Apo-J), NGAL and TIMP-1, in a single well using Luminex xMAP technology to determine the potential nephrotoxicity during drug studies. Samples were measured according to the manufacturer's protocol.

For evaluation of T helper response, the Th Complete 14-Plex Rat ProcartaPlex™ Panel (Invitrogen # EPX140-30120-901) was used. This panel allows the analysis of 14 protein targets in a single well using Luminex xMAP technology. Targets are IL-1α; G-CSF; IL-10; IL-17A; IL-1β; IL-6; TNFα; IL-4; GM-CSF; IFNγ; IL-2; IL-5; IL-13; IL-12p70. Samples were

measured according to the manufacturer's protocol on Bio-Plex 200 Systems (Bio-Rad, Hercules, CA, USA).

4.6. Behavioural Tests

To assess the behavioural effect of 4MU, 2 tests were selected. The rotarod was used to assess motor performance and motor coordination and the forelimb grip strength test aimed to test neuromuscular functions by determining the maximal force developed by a rat. Both tests were used to investigate whether 4MU has any effect on motor functions and/or joint mobility, and were performed after 10 weeks of 4MU treatment in all three groups and 9 weeks after 4MU treatment in the wash-out group. Prior to the rotarod (ROTA-ROD 47700, UGO BASILE S.R.I.) training session, rats were habituated to remain on a stationary drum for 60 s and pretrained at 5 rpm for 120 s. In the testing phase, animals were tested for 300 s with increasing acceleration from 5 to 10 rpm for the first 180 s and then for additional 120 s with acceleration of 10 rpm on three different days following training. The time at which the rat fell off the rotating bar was recorded. For the forelimb grip strength, an instrument (BSGT2S; Harvard Apparatus, Holliston, MA, USA) was used. The researcher pulled horizontally on the tail of the rat, which was gripping a metal grid attached to the monitoring device. The force applied to the grid before the rat lost its grip was recorded as the maximal muscle force. The test was repeated on three different days over the course of one week. Data from 4-MU treated group and wash-out group were collected independently.

4.7. Histopathological Evaluation

For histopathological evaluation, spleen, liver, kidney, heart and small intestine were collected after transcardial perfusion and fixed for 24 h in 4% paraformaldehyde in 0.1 M PBS. Formalin-fixed paraffin-embedded (FFPE) samples were cut into 5 µm thin slices on a Leica RM2255 (Leica Biosystems Nussloch GmbH, Nußloch, Germany) microtome, placed on standard slides (Bammed s.r.o, Czech Republic) and stained with haematoxylin–eosin (DiaPath, Martinengo, Italy).

4.8. Bone Marrow Evaluation

Bone marrow was collected from tibia. Tibias were cleaned of fat, muscles and tendons. Then, the tibial heads were cut off with scissors and the bone marrow was flushed out of the bone with a 10 mL syringe. The bone marrow suspension was placed on one side of a microscope slide, gently spread with a second slide to form a thin film on the slide and fixed with methanol. Cells were stained using Pappenheim panoptic staining, a combination of May–Grünwald staining and Giemsa staining. This staining method allows the visualisation of basophilic, neutrophilic and eosinophilic blood structures. The May–Grünwald solution contains two dyes, eosin and methylene blue. We first allowed the methanol-fixed bone marrow smear to dry. May–Grünwald solution was then added (5 min). Next, distilled water was used to remove the May–Grünwald solution (5 min). Following this step, Romanowsky–Giemsa stain was added (10 min) and then washed with distilled water. The microscope slides were then allowed to dry, and the blood smear was observed with a microscope (Olympus CX41, Shinjuku City, Tokyo, Japan) using 100× objective lens and immersion oil. The relative number of different elements in the smears was then determined by counting and classifying 1000 cells in the bone marrow per smear.

4.9. Biomechanical Testing

4.9.1. Conditions and Equipment

Tested tissues were frozen for preservation. After thawing, the specimens were hydrated in a physiological saline solution at 8 °C for a period of 24 h before the experiment. The specimens were left at room temperature (23 ± 2 °C) for 2 h before the test. The MTS Mini Bionix 858.02 biomechanical servohydraulic testing system (MTS, Minnesota, USA) with load cell with a measuring range of 0–500 N (detector error max. 0.05%, e.g., 0.08 N

error when 160 N is applied) was used for the three-point bending test, as well as the tensile test of skin and the tensile test of tendons.

4.9.2. Tensile Tests of Skin

The mechanical properties were evaluated by uniaxial tensile tests of rectangular strips of skin (width of the samples was 8 mm; the thickness was 0.8–1.0 mm). The experimental methodology was based on the determination of the ultimate force during the tensile test and the modulus of elasticity of the skin at a defined deformation. The evaluation parameters were Young' tensile modulus E determined at two values of longitudinal relative deformation, 5% (E_5) and 10% (E_{10}). These values were obtained as the tangent direction of the linear region of the load curve of the dependence of the true stress on the relative deformation. The biomechanical servohydraulic testing system MTS Mini Bionix 858.02 and pneumatic jaws were used for the tensile test. Using the contrast marks on the surface of the specimens, the video extensometer automatically determined the reference length and elongation of the specimens. The specimens were attached to the pneumatic jaws and loaded at a constant rate of 20.0 mm/min until destruction.

4.9.3. Tensile Test of Tendons

An evaluation of the mechanical properties of the rat tendons was carried out by destructive tensile tests in order to evaluate their strength. Rat tendon specimens were delivered in a BTM (bone to muscle) disposition, i.e., the tendon was dissected on one side with part of the muscle and on the other side with part of the bone. This configuration allowed for a secure setting in the pneumatic jaws during testing. The muscle was frozen by soaking in liquid nitrogen for 5 s before testing each sample. Care was taken to ensure that the tendon did not freeze with the muscle. The MTS Mini Bionix 858.02 biomechanical servohydraulic testing system and pneumatic jaws were used for the tensile test. The tendons were fixed between two metal clamps mounted in pneumatic clamp grips, ensuring a constant downforce and tough, stable attachment of the samples during cross-sectional changes. The grips were equipped with diamond-like apexes. The samples were loaded at a constant speed of 10.0 mm/min until destruction. The evaluation parameters were the maximum force and maximum stress (i.e., strength), strength was calculated from the equation $\sigma_{max} = F_{max}/S$ (MPa).

4.9.4. Statistical Analysis of Data

Data are expressed as means ± SEM of n independent measurements. The significance of the difference between the means of two or three groups of data was evaluated using one-way ANOVA (HABP and ACAN intensity, behavioural test, proteomic, bone marrow evaluation, biomechanical testing) or two-way ANOVA (CS-56 and HABP intensity, haematological, serological and biochemical parameters, glycosuria and urinary proteins). A p value < 0.05 was considered statistically significant. Statistical analysis was performed with GraphPad Prism 9 software (version 9.3.0).

5. Conclusions

Our results show that 4MU at a dose of 1.2 g/kg/day after a 10-week treatment reduces whole-body HA levels; however, the current dose did not lead to any serious adverse effects. If any deviations from the reference values occurred, they normalised after a 9-week wash-out period in Wistar rats. Our findings indicate that 4MU could be considered as a long-term treatment at a dose of 1.2 g/kg/day. However, we did not address the possible behavioural changes causing PNN alteration in brain regions associated with psychiatric disorders such as schizophrenia, autism spectrum disorders and mood disorders. More detailed studies would be required to further characterise potential psychiatric adverse effects.

Supplementary Materials: The supporting information can be downloaded at: https://www.mdpi.com/article/10.3390/ijms24043799/s1.

Author Contributions: Conceptualization, J.C.F.K., P.J. and L.M.U.; methodology, R.S., K.T., Š.K., P.M., M.P., J.C.F.K., P.J. and L.M.U.; validation, K.Š., D.M. and K.K.; formal analysis, K.Š., K.K., R.S., K.T. and I.V.; investigation, K.Š., D.M., K.K. and I.V.; resources, J.C.F.K. and P.J.; data curation, K.Š., D.M., K.K., R.S., K.T., P.M., M.P., J.C.F.K. and L.M.U.; writing—original draft preparation, K.Š. and L.M.U.; writing—review and editing, J.C.F.K., P.J. and L.M.U.; supervision, R.S, K.T., P.M., M.P., J.C.F.K., P.J. and L.M.U.; project administration, J.C.F.K., P.J. and L.M.U.; funding acquisition, J.C.F.K., P.J. and L.M.U. All authors have read and agreed to the published version of the manuscript.

Funding: This research was supported by the Center of Reconstruction Neuroscience—NEURORECON CZ.02.1.01/0.0/0.0/15_003/0000419 (to L.M.U., P.J. and J.C.F.K.), the Czech Science Agency 19-10365S (to P.J. and J.C.F.K.), and Wings for Life (WFL-UK-008-15) and Medical Research Council UK (confidence in concept MC-PC-16050 and project grant MR/S011110/1) to J.C.F.K.

Institutional Review Board Statement: The animal study protocols were approved by the ethical committee of the Institute of Experimental medicine of ASCR and performed in accordance with Law No. 77/2004 of the Czech Republic (approval number: 13/2020, approved in 2020).

Informed Consent Statement: Not applicable.

Data Availability Statement: Data are available in the Supplementary files.

Acknowledgments: Microscopy was performed at the Microscopy Service Centre of the Institute of Experimental Medicine CAS supported by the MEYS CR (project Czech-Bioimaging).

Conflicts of Interest: Kwok has a patent 'Treatment of Conditions of the Nervous System' (PCT/EP2020/079979) issued.

Abbreviations

4MU	4-methylumbelliferone
ACAN	Aggrecan
ALP	Alkaline phosphatase
ALT	Alanine transaminase
Apo-J	Apolipoprotein J
AST	Aspartate transaminase
BTM	Bone to muscle (deposition)
CNS	Central nervous system
CS-56	Anti-chondroitin sulphate antibody
CS	Chondroitin sulphate
CSPGs	Chondroitin sulphate proteoglycans
Cys	Cystatin C
DAPI	4′,6-diamidino-2-phenylindole, dihydrochloride
ECM	Extracellular matrix
FFPE	Formalin-fixed paraffin-embedded
GAG	Glycosaminoglycans
G-CSF	Granulocyte colony-stimulating factor
GlcA	D-glucuronic acid
GM-CSF	Granulocyte macrophage colony-stimulating factor
HA	Hyaluronan/hyaluronic acid
HAS	Hyaluronan synthase
HABP	Hyaluronan-binding protein
IFNγ	Interferon gamma
IL10	Interleukin 10
IL12p70	Interleukin 12p70
IL13	Interleukin 13
IL17a	Interleukin 17A
IL1α	Interleukin 1 alpha
IL1β	Interleukin 1 beta

IL2	Interleukin 2
IL4	Interleukin 4
IL5	Interleukin 5
IL6	Interleukin 6
IL10	Interleukin 10
JAK	Janus kinase
NGAL	Neutrophil gelatinase-associated lipocalin
PBS	Phosphate-buffered saline
PNNs	Perineuronal nets
RT	Room temperature
SCI	Spinal cord injury
STAT3	Signal transducer and activator of transcription 3
TIMP-1	Tissue inhibitor of metalloproteinases 1
TNFα	Tumour necrosis factor alpha
UDP-GlcA	UDP-glucuronic acid

References

1. Klos, C.; Paumgartner, G.; Reichen, J. Cation-anion gap and choleretic properties of rat bile. *Am. J. Physiol. -Endocrinol. Metab.* **1979**, *236*, E434. [CrossRef]
2. Elferink, R.P.J.O.; Tytgat, G.N.J.; Groen, A.K. The role of mdr2 P-glycoprotein in hepatobiliary lipid transport. *FASEB J.* **1997**, *11*, 19–28. [CrossRef]
3. Takeda, S.; Aburada, M. The choleretic mechanism of coumarin compounds and phenolic compounds. *J. Pharm.* **1981**, *4*, 724–734. [CrossRef] [PubMed]
4. Nagy, N.; Gurevich, I.; Kuipers, H.F.; Ruppert, S.M.; Marshall, P.L.; Xie, B.J.; Sun, W.; Malkovskiy, A.V.; Rajadas, J.; Grandoch, M.; et al. 4-Methylumbelliferyl glucuronide contributes to hyaluronan synthesis inhibition. *J. Biol. Chem.* **2019**, *294*, 7864–7877. [CrossRef]
5. Dubisova, J.; Burianova, J.S.; Svobodova, L.; Makovicky, P.; Martinez-Varea, N.; Cimpean, A.; Fawcett, J.W.; Kwok, J.C.; Kubinova, S. Oral treatment of 4-methylumbelliferone reduced perineuronal nets and improved recognition memory in mice. *Brain Res. Bull.* **2022**, *181*, 144–156. [CrossRef]
6. Irvine, S.F.; Gigout, S.; Štěpánková, K.; Varea, N.M.; Urdzíková, L.M.; Jendelová, P.; Kwok, J.C.F. 4-Methylumbelliferone enhances neuroplasticity in the central nervous system: Potential oral treatment for SCI. *bioRxiv* **2023**, arXiv:2023.01.23.525137.
7. Nagy, N.; Kuipers, H.F.; Frymoyer, A.R.; Ishak, H.D.; Bollyky, J.B.; Wight, T.N.; Bollyky, P.L. 4-Methylumbelliferone Treatment and Hyaluronan Inhibition as a Therapeutic Strategy in Inflammation, Autoimmunity, and Cancer. *Front. Immunol.* **2015**, *6*, 123. [CrossRef] [PubMed]
8. Stepankova, K.; Chudickova, M.; Simkova, Z.; Martinez-Varea, N.; Kubinova, S.; Urdzikova, L.; Jendelova, P.; Kwok, J.C. Oral administration of 4-methylumbelliferone reduces glial scar and promotes anatomical plasticity. *bioRxiv* **2023**, arXiv:2023.02.02.526565.
9. Sorg, B.A.; Berretta, S.; Blacktop, J.M.; Fawcett, J.W.; Kitagawa, H.; Kwok, J.C.; Miquel, M. Casting a Wide Net: Role of Perineuronal Nets in Neural Plasticity. *J. Neurosci.* **2016**, *36*, 11459–11468. [CrossRef]
10. Wang, D.; Fawcett, J. The perineuronal net and the control of CNS plasticity. *Cell Tissue Res.* **2012**, *349*, 147–160. [CrossRef]
11. Ghorbani, S.; Yong, V.W. The extracellular matrix as modifier of neuroinflammation and remyelination in multiple sclerosis. *Brain* **2021**, *144*, 1958–1973. [CrossRef] [PubMed]
12. Yong, N.; Guoping, C. Upregulation of matrix metalloproteinase-9 dependent on hyaluronan synthesis after sciatic nerve injury. *Neurosci. Lett.* **2008**, *444*, 259–263. [CrossRef] [PubMed]
13. Kuipers, H.F.; Nagy, N.; Ruppert, S.M.; Sunkari, V.G.; Marshall, P.L.; A Gebe, J.; Ishak, H.D.; Keswani, S.G.; Bollyky, J.; Frymoyer, A.R.; et al. The pharmacokinetics and dosing of oral 4-methylumbelliferone for inhibition of hyaluronan synthesis in mice. *Clin. Exp. Immunol.* **2016**, *185*, 372–381. [CrossRef] [PubMed]
14. Garrett, E.R.; Venitz, J.; Eberst, K.; Cerda, J.J. Pharmacokinetics and bioavailabilities of hymecromone in human volunteers. *Biopharm Drug Dispos* **1993**, *14*, 13–39. [CrossRef] [PubMed]
15. Morita, K.; Sugiyama, Y.; Hanano, M. Pharmacokinetic study of 4-methylumbelliferone in rats: Influence of dose on its first-pass hepatic elimination. *J. Pharm.* **1986**, *9*, 117–124. [CrossRef]
16. Kobayashi, T.; Chanmee, T.; Itano, N. Hyaluronan: Metabolism and Function. *Biomolecules* **2020**, *10*, 1525. [CrossRef]
17. David, S.; Hamilton, J.P. Drug-induced Liver Injury. *US Gastroenterol. Hepatol. Rev.* **2010**, *6*, 73–80. [PubMed]
18. Hoffmann, R.M.; Schwarz, G.; Pohl, C.; Ziegenhagen, D.J.; Kruis, W. [Bile acid-independent effect of hymecromone on bile secretion and common bile duct motility]. *Dtsch. Med. Wochenschr. (1946)* **2005**, *130*, 1938–1943. [CrossRef] [PubMed]
19. Makris, K.; Markou, N.; Evodia, E.; Dimopoulou, E.; Drakopoulos, I.; Ntetsika, K.; Rizos, D.; Baltopoulos, G.; Haliassos, A. Urinary neutrophil gelatinase-associated lipocalin (NGAL) as an early marker of acute kidney injury in critically ill multiple trauma patients. *Clin. Chem. Lab. Med.* **2009**, *47*, 79–82. [CrossRef]

20. Zhang, X.; Chen, X.; Hong, Q.; Lin, H.; Zhu, H.; Liu, Q.; Wang, J.; Xie, Y.; Shang, X.; Shi, S.; et al. TIMP-1 promotes age-related renal fibrosis through upregulating ICAM-1 in human TIMP-1 transgenic mice. *J. Gerontol. Ser. A Biol. Sci. Med. Sci.* **2006**, *61*, 1130–1143. [CrossRef]
21. Goncharova, V.; Serobyan, N.; Iizuka, S.; Schraufstatter, I.; de Ridder, A.; Povaliy, T.; Wacker, V.; Itano, N.; Kimata, K.; Orlovskaja, I.A.; et al. Hyaluronan expressed by the hematopoietic microenvironment is required for bone marrow hematopoiesis. *J. Biol. Chem.* **2012**, *287*, 25419–25433. [CrossRef] [PubMed]
22. Sikes, K.J.; Renner, K.; Li, J.; Grande-Allen, K.J.; Connell, J.P.; Cali, V.; Midura, R.J.; Sandy, J.D.; Plaas, A.; Wang, V.M. Knockout of hyaluronan synthase 1, but not 3, impairs formation of the retrocalcaneal bursa. *J. Orthop. Res. Off. Publ. Orthop. Res. Soc.* **2018**, *36*, 2622–2632. [CrossRef] [PubMed]
23. Papakonstantinou, E.; Roth, M.; Karakiulakis, G. Hyaluronic acid: A key molecule in skin aging. *Dermato-Endocrinol.* **2012**, *4*, 253–258. [CrossRef]
24. Nakamura, T.; Takagaki, K.; Shibata, S.; Tanaka, K.; Higuchi, T.; Endo, M. Hyaluronic-Acid-Deficient Extracellular Matrix Induced by Addition of 4-Methylumbelliferone to the Medium of Cultured Human Skin Fibroblasts. *Biochem. Biophys. Res. Commun.* **1995**, *208*, 470–475. [CrossRef]
25. Kakizaki, I.; Kojima, K.; Takagaki, K.; Endo, M.; Kannagi, R.; Ito, M.; Maruo, Y.; Sato, H.; Yasuda, T.; Mita, S.; et al. A novel mechanism for the inhibition of hyaluronan biosynthesis by 4-methylumbelliferone. *J. Biol. Chem.* **2004**, *279*, 33281–33289. [CrossRef] [PubMed]
26. Monslow, J.; Govindaraju, P.; Puré, E. Hyaluronan—A functional and structural sweet spot in the tissue microenvironment. *Front Immunol.* **2015**, *6*, 231. [CrossRef]
27. Vigetti, D.; Rizzi, M.; Viola, M.; Karousou, E.; Genasetti, A.; Clerici, M.; Bartolini, B.; Hascall, V.C.; De Luca, G.; Passi, A. The effects of 4-methylumbelliferone on hyaluronan synthesis, MMP2 activity, proliferation, and motility of human aortic smooth muscle cells. *Glycobiology* **2009**, *19*, 537–546. [CrossRef]
28. Dicker, K.T.; Gurski, L.A.; Pradhan-Bhatt, S.; Witt, R.L.; Farach-Carson, M.C.; Jia, X. Hyaluronan: A simple polysaccharide with diverse biological functions. *Acta Biomater.* **2014**, *10*, 1558–1570. [CrossRef] [PubMed]
29. Peters, A.; Sherman, L.S. Diverse Roles for Hyaluronan and Hyaluronan Receptors in the Developing and Adult Nervous System. *Int. J. Mol. Sci.* **2020**, *21*, 5988. [CrossRef]
30. Smith, C.C.; Mauricio, R.; Nobre, L.; Marsh, B.; Wüst, R.C.; Rossiter, H.B.; Ichiyama, R.M. Differential regulation of perineuronal nets in the brain and spinal cord with exercise training. *Brain Res Bull.* **2015**, *111*, 20–26. [CrossRef]
31. Pantazopoulos, H.; Berretta, S. In Sickness and in Health: Perineuronal Nets and Synaptic Plasticity in Psychiatric Disorders. *Neural Plast.* **2016**, *2016*, 9847696. [CrossRef]
32. De la Motte, C.A.; Kessler, S.P. The role of hyaluronan in innate defense responses of the intestine. *Int. J. Cell Biol.* **2015**, *2015*, 481301. [CrossRef]
33. Galdi, F.; Pedone, C.; McGee, C.A.; George, M.; Rice, A.B.; Hussain, S.S.; Vijaykumar, K.; Boitet, E.R.; Tearney, G.J.; McGrath, J.A.; et al. Inhaled high molecular weight hyaluronan ameliorates respiratory failure in acute COPD exacerbation: A pilot study. *Respir. Res.* **2021**, *22*, 30. [CrossRef]
34. Papanastasopoulou, C.; Papastamataki, M.; Karampatsis, P.; Anagnostopoulou, E.; Papassotiriou, I.; Sitaras, N. Cardiovascular Risk and Serum Hyaluronic Acid: A Preliminary Study in a Healthy Population of Low/Intermediate Risk. *J. Clin. Lab. Anal.* **2017**, *31*, e22010. [CrossRef]
35. Amir, A.; Kim, S.; Stecco, A.; Jankowski, M.P.; Raghavan, P. Hyaluronan homeostasis and its role in pain and muscle stiffness. *PM R J. Inj. Funct. Rehabil.* **2022**, *14*, 1490–1496. [CrossRef]
36. Kaux, J.F.; Samson, A.; Crielaard, J.M. Hyaluronic acid and tendon lesions. *Muscles Ligaments Tendons J.* **2015**, *5*, 264–269. [CrossRef] [PubMed]
37. Tamer, T.M. Hyaluronan and synovial joint: Function, distribution and healing. *Interdiscip. Toxicol.* **2013**, *6*, 111–125. [CrossRef] [PubMed]
38. Rivers, D.A.; Stern, R. Hyaluronan and the Process of Aging in Skin. In *Textbook of Aging Skin*; Farage, M., Miller, K., Maibach, H., Eds.; Springer: Berlin, Heidelberg, 2017.
39. Hansen, J.F.; Christiansen, K.M.; Staugaard, B.; Moessner, B.K.; Lillevang, S.; Krag, A.; Christensen, P.B. Combining liver stiffness with hyaluronic acid provides superior prognostic performance in chronic hepatitis C. *PLoS ONE* **2019**, *14*, e0212036. [CrossRef]
40. Katarey, D.; Verma, S. Drug-induced liver injury. *Clin. Med.* **2016**, *16* (Suppl. 6), s104–s109. [CrossRef]
41. Kakehi, K.; Kinoshita, M.; Yasueda, S.-i. Hyaluronic acid: Separation and biological implications. *J. Chromatogr. B* **2003**, *797*, 347–355. [CrossRef] [PubMed]
42. Toole, B.P. Hyaluronan: From extracellular glue to pericellular cue. *Nat. Rev. Cancer* **2004**, *4*, 528–539. [CrossRef]
43. Fenderson, B.A.; Stamenkovic, I.; Aruffo, A. Localization of hyaluronan in mouse embryos during implantation, gastrulation and organogenesis. *Differ. Res. Biol. Divers.* **1993**, *54*, 85–98.
44. Tammi, M.; Seppälä, P.O.; Lehtonen, A.; Möttönen, M. Connective tissue components in normal and atherosclerotic human coronary arteries. *Atherosclerosis* **1978**, *29*, 191–194. [CrossRef] [PubMed]
45. Smadja-Joffe, F.; Legras, S.; Girard, N.; Li, Y.; Delpech, B.; Bloget, F.; Morimoto, K.; Le Bousse-Kerdilès, C.; Clay, D.; Jasmin, C.; et al. CD44 and hyaluronan binding by human myeloid cells. *Leuk. Lymphoma* **1996**, *21*, 407–420. [CrossRef] [PubMed]

46. Drózdz, M.; Kula, B.; Wardas, M.; Weglarz, L. Hyaluronic acid content and hyaluronidase activity in liver and spleen of rats with hydralazine-induced collagen-like syndrome. *Biomed. Biochim. Acta* **1988**, *47*, 247–250. [PubMed]
47. Andreutti, D.; Geinoz, A.; Gabbiani, G. Effect of hyaluronic acid on migration, proliferation and alpha-smooth muscle actin expression by cultured rat and human fibroblasts. *J. Submicrosc. Cytol. Pathol.* **1999**, *31*, 173–177.
48. Klamer, S.; Voermans, C. The role of novel and known extracellular matrix and adhesion molecules in the homeostatic and regenerative bone marrow microenvironment. *Cell Adhes. Migr.* **2014**, *8*, 563–577. [CrossRef]
49. Köpke-Aguiar, L.A.; Martins, J.R.; Passerotti, C.C.; Toledo, C.F.; Nader, H.B.; Borges, D.R. Serum hyaluronic acid as a comprehensive marker to assess severity of liver disease in schistosomiasis. *Acta Trop.* **2002**, *84*, 117–126. [CrossRef]
50. Malakouti, M.; Kataria, A.; Ali, S.K.; Schenker, S. Elevated Liver Enzymes in Asymptomatic Patients-What Should I Do? *J. Clin. Transl. Hepatol.* **2017**, *5*, 394–403. [CrossRef] [PubMed]
51. Dufour, D.R.; Lott, J.A.; Nolte, F.S.; Gretch, D.R.; Koff, R.S.; Seeff, L.B. Diagnosis and monitoring of hepatic injury. II. Recommendations for use of laboratory tests in screening, diagnosis, and monitoring. *Clin. Chem.* **2000**, *46*, 2050–2068. [CrossRef]
52. Miura, Y. [Aspartate aminotransferase (AST) and alanine aminotransferase (ALT)]. *Nihon Rinsho Jpn. J. Clin. Med.* **1995**, *53 Pt 1*, 266–271.
53. Kvietys, P.R.; Granger, D.N. Role of intestinal lymphatics in interstitial volume regulation and transmucosal water transport. *Ann. N. Y. Acad. Sci.* **2010**, *1207* (Suppl. 1), E29–E43. [CrossRef] [PubMed]
54. De la Motte, C.A.; Hascall, V.C.; Drazba, J.; Bandyopadhyay, S.K.; Strong, S.A. Mononuclear leukocytes bind to specific hyaluronan structures on colon mucosal smooth muscle cells treated with polyinosinic acid:polycytidylic acid: Inter-alpha-trypsin inhibitor is crucial to structure and function. *Am. J. Pathol.* **2003**, *163*, 121–133. [CrossRef]
55. Kaul, A.; Singampalli, K.L.; Parikh, U.M.; Yu, L.; Keswani, S.G.; Wang, X. Hyaluronan, a double-edged sword in kidney diseases. *Pediatr. Nephrol.* **2022**, *37*, 735–744. [CrossRef] [PubMed]
56. Colombaro, V.; Declèves, A.E.; Jadot, I.; Voisin, V.; Giordano, L.; Habsch, I.; Nonclercq, D.; Flamion, B.; Caron, N. Inhibition of hyaluronan is protective against renal ischaemia-reperfusion injury. *Nephrol. Dial. Transplant. Off. Publ. Eur. Dial. Transpl. Assoc.-Eur. Ren. Assoc.* **2013**, *28*, 2484–2493. [CrossRef] [PubMed]
57. Fraser, J.R.; Laurent, T.C.; Laurent, U.B. Hyaluronan: Its nature, distribution, functions and turnover. *J. Intern. Med.* **1997**, *242*, 27–33. [CrossRef]
58. Laurent, C.; Johnson-Wells, G.; Hellström, S.; Engström-Laurent, A.; Wells, A.F. Localization of hyaluronan in various muscular tissues. A morphological study in the rat. *Cell Tissue Res.* **1991**, *263*, 201–205. [CrossRef]
59. Stecco, C.; Stern, R.; Porzionato, A.; Macchi, V.; Masiero, S.; Stecco, A.; De Caro, R. Hyaluronan within fascia in the etiology of myofascial pain. *Surg. Radiol. Anat. SRA* **2011**, *33*, 891–896. [CrossRef]
60. Purslow, P.P. Muscle fascia and force transmission. *J. Bodyw. Mov. Ther.* **2010**, *14*, 411–417. [CrossRef]
61. Hunter, S.K.; Pereira, H.M.; Keenan, K.G. The aging neuromuscular system and motor performance. *J. Appl. Physiol.* **2016**, *121*, 982–995. [CrossRef]
62. Stern, R.; Maibach, H.I. Hyaluronan in skin: Aspects of aging and its pharmacologic modulation. *Clin. Dermatol.* **2008**, *26*, 106–122. [CrossRef] [PubMed]
63. Longaker, M.T.; Chiu, E.S.; Adzick, N.S.; Stern, M.; Harrison, M.R.; Stern, R. Studies in fetal wound healing. V. A prolonged presence of hyaluronic acid characterizes fetal wound fluid. *Ann. Surg.* **1991**, *213*, 292–296. [CrossRef]
64. Schachtschabel, D.O.; Wever, J. Age-related decline in the synthesis of glycosaminoglycans by cultured human fibroblasts (WI-38). *Mech. Ageing Dev.* **1978**, *8*, 257–264. [CrossRef] [PubMed]
65. Girish, K.S.; Kemparaju, K. The magic glue hyaluronan and its eraser hyaluronidase: A biological overview. *Life Sci.* **2007**, *80*, 1921–1943. [CrossRef]
66. Chen, L.; Deng, H.; Cui, H.; Fang, J.; Zuo, Z.; Deng, J.; Li, Y.; Wang, X.; Zhao, L. Inflammatory responses and inflammation-associated diseases in organs. *Oncotarget* **2018**, *9*, 7204–7218. [CrossRef] [PubMed]
67. Horton, M.R.; Burdick, M.D.; Strieter, R.M.; Bao, C.; Noble, P.W. Regulation of hyaluronan-induced chemokine gene expression by IL-10 and IFN-gamma in mouse macrophages. *J. Immunol.* **1998**, *160*, 3023–3030. [CrossRef]
68. King, A.; Balaji, S.; Le, L.D.; Crombleholme, T.M.; Keswani, S.G. Regenerative Wound Healing: The Role of Interleukin-10. *Adv. Wound Care* **2014**, *3*, 315–323. [CrossRef]

scientific reports

Check for updates

OPEN

Low oral dose of 4-methylumbelliferone reduces glial scar but is insufficient to induce functional recovery after spinal cord injury

Kateřina Štepánková[1,2,5]✉, Milada Chudíčková[1,5], Zuzana Šimková[1], Noelia Martinez-Varea[1,2], Šárka Kubinová[1,3], Lucia Machová Urdzíková[1,2]✉, Pavla Jendelová[1,2]✉ & Jessica C. F. Kwok[1,4]✉

Spinal cord injury (SCI) induces the upregulation of chondroitin sulfate proteoglycans (CSPGs) at the glial scar and inhibits neuroregeneration. Under normal physiological condition, CSPGs interact with hyaluronan (HA) and other extracellular matrix on the neuronal surface forming a macromolecular structure called perineuronal nets (PNNs) which regulate neuroplasticity. 4-methylumbelliferone (4-MU) is a known inhibitor for HA synthesis but has not been tested in SCI. We first tested the effect of 4-MU in HA reduction in uninjured rats. After 8 weeks of 4-MU administration at a dose of 1.2 g/kg/day, we have not only observed a reduction of HA in the uninjured spinal cords but also a down-regulation of CS glycosaminoglycans (CS-GAGs). In order to assess the effect of 4-MU in chronic SCI, six weeks after Th8 spinal contusion injury, rats were fed with 4-MU or placebo for 8 weeks in combination with daily treadmill rehabilitation for 16 weeks to promote neuroplasticity. 4-MU treatment reduced the HA synthesis by astrocytes around the lesion site and increased sprouting of 5-hydroxytryptamine fibres into ventral horns. However, the current dose was not sufficient to suppress CS-GAG up-regulation induced by SCI. Further adjustment on the dosage will be required to benefit functional recovery after SCI.

Abbreviations

4-MU	4-Methylumbelliferone
5-HT	5-Hydroxytryptamine
ACAN	Aggrecan
ChAT	Choline acetyltransferase
ChABC	Chondroitinase ABC
CNS	Central nervous system
CS-GAGs	Chondroitin sulfate glycosaminoglycans
CSPGs	Chondroitin sulfate proteoglycans
HA	Hyaluronan
HABP	Hyaluronan binding protein
HASs	Hyaluronan synthases
UDP-GlcA	UDP-glucuronic acid
UGT	UDP-glucuronyl transferase
PNNs	Perineuronal nets

[1]Institute of Experimental Medicine, Czech Academy of Sciences, Vídeňská, 1083 Prague, Czech Republic. [2]Department of Neuroscience, Charles University, Second Faculty of Medicine, 15006 Prague, Czech Republic. [3]Institute of Physics, Czech Academy of Sciences, 182 21 Prague, Czech Republic. [4]Faculty of Biological Sciences, University of Leeds, Leeds LS2 9JT, UK. [5]These authors contributed equally: Kateřina Štepánková and Milada Chudíčková. ✉email: katerina.stepankova@iem.cas.cz; lucia.machova@iem.cas.cz; pavla.jendelova@iem.cas.cz; j.kwok@leeds.ac.uk

SCI	Spinal cord injury
WFA	*Wisteria floribunda* Agglutinin

Spinal cord injury (SCI) is a damage to the spinal cord that causes partial or complete loss of control of locomotor and sensory functions[1]. SCI itself is a dynamic process starting immediately after the injury when tissue damage is continued with haemorrhage, inflammation, as well as oedema. The acute phase includes initial trauma followed by spinal cord ischemia, cell excitotoxicity, ion dysregulation, and free radical-mediated peroxidation[2]. These processes initiate a complex secondary injury cascade leading to changes in structural architecture of the spinal cord characterised by the chronic phase. Chronic phase begins 6 months after SCI in human and continues throughout the lifetime of the patient. It is characterized by the stabilization of the lesion including scar formation accompanied by alterations in neural circuitries[3]. As there is no successful regenerative treatment available, most patients remain in the chronic state for the rest of their life.

Adult central nervous system (CNS) has relatively poor regeneration capacity caused by both the extrinsic inhibitory environment after injury (such as glial scar and myelin-associated inhibitors) and the intrinsic poor regeneration ability of the neurons themselves[4,5]. While these extrinsic and intrinsic factors co-ordinate to maintain the stability of the neural networks in a healthy state, they rapidly become the major obstruction to regeneration post-injury[6]. Perineuronal nets (PNNs) are extracellular matrix (ECM) structures enwrapping a subpopulation of neurons in the CNS and play a crucial role in plasticity regulation during postnatal development and post traumatic regeneration[7,8]. PNNs form at the end of the critical period in the CNS and terminate developmental neuroplasticity. PNNs mature by early adulthood[9] and stabilize synaptic contacts and are dynamically maintained during the lifespan[9–11]. In spinal cord, PNNs mainly surround motoneurons in the ventral horns[12–14] that are directly responsible for the motor activity[15]. PNNs are composed of a multitude of neural ECM components where chondroitin sulfate proteoglycans (CSPGs) and hyaluronan (HA) are the major constituents[8,16,17].

Degradation of PNNs reactivates juvenile-like state of plasticity which enables axon sprouting and regeneration of function by synaptogenesis and experience-dependent synaptic plasticity after SCI[18]. Enzymatic removal of PNNs through chondroitinase ABC (ChABC), that digests chondroitin sulfate glycosaminoglycan (CS-GAG) chains on CSPGs, has shown to reopen a critical window for plasticity enhancement and promote functional recovery in multiple SCI models[19,20]. Moreover, when ChABC is combined with rehabilitation, the effect of ChABC treatment is enhanced as compared to non-rehabilitating animals[21,22]. CSPG synthesis inhibitors, such as fluorosamine and its analogues, have also been shown to reduce CS-GAG level and accelerate remyelination following focal demyelination in mice[1,23]. These results suggest that CSPG synthesis inhibitors are possible approaches to enable axonal regeneration after CNS injury.

We have recently reported the use of a small molecule 4-methylumbelliferone (4-MU) to down-regulate PNNs and re-activate neuroplasticity for memory enhancement[24]. 4-MU is a known inhibitor to HA synthesis[25,26]. Previous work has shown that 4-MU inhibits the production of UDP-glucuronic acid (UDP-GlcA)[27], a key substrate for HA production, and the expression of hyaluronan synthases (HASs), UDP-glucose-pyrophosphorylase (an enzyme for the biosynthesis of UDP-glucose) and UDP-glucose-dehydrogenase (an enzyme that converts UDP-glucose into UDP-glucuronic acid)[28,29]. Interestingly, UDP-GlcA is also a substrate for the synthesis of CS, as well as some other GAGs including dermatan and heparan sulfates. The effect of 4-MU in general GAG synthesis has yet to be clarified in vivo.

Our previous observation of PNN down-regulation by 4-MU prompts us to ask the question if 4-MU would be effective in down-regulating the inhibitory ECM (i.e. ECM molecules, such as proteoglycans, which are up-regulated after injury and restricting axonal growth) in the glial scar after SCI. Here, we aimed to evaluate the biochemical and histological changes in the injured spinal cord after long-term 4-MU treatment in rats and to evaluate the effect of this molecule on anatomical changes in the spinal cord after chronic SCI. Histological staining of PNNs using *Wisteria floribunda agglutinin* (WFA) and anti-aggrecan antibody (ACAN, a CSPG) shows PNN down-regulation in 4-MU-treated group, and that the staining recovers in wash-out group. We also observed that the long-term 4-MU treatment leads to a significant reduction in the glial scar and promotes the sprouting of serotonergic fibres above and below the lesion.

Results

4-MU decreases GAG synthesis and PNN in uninjured spinal cord

We first investigated the effect of 4-MU in the down-regulation of GAGs in the CNS and its effect on PNNs, with and without treadmill training which is a common rehabilitation. We tested the efficacy of a lower dose at 1.2 g/kg/day weight aiming to minimize the 4-MU consumption for potential adverse effects of long-term treatment for SCI[30]. A timeline for the feeding regime can be found in Fig. 1 (Non-SCI).

Adult rats were fed with 4-MU at a dose of 1.2 g/kg/day daily for 8-weeks, and some of them were then subjected to 2 months of wash-out. We extracted the GAGs from the dissected spinal cords and quantified the total amount for HA and GAGs using turbidity assay[31] (Fig. 2A). The results showed that 4-MU treatment alone (0.09 ± 0.81 mg/g; $n = 4$; $p = 0.0086$) and 4-MU plus daily treadmill training (0.17 ± 0.16 mg/g; $n = 4$; $p = 0.0113$) have significantly reduced the level of GAGs compared to placebo group (2.02 ± 0.70 mg/g; $n = 4$). Rehabilitation did not affect the effectiveness of 4-MU in down-regulating GAG synthesis in treated animals. Interestingly, daily treadmill training alone also showed a modest, but non-significant reduction in GAGs level when combined with placebo (1.06 ± 0.16 mg/g; n = 4; $p = 0.2555$) suggesting that rehabilitation (or training) can independently reduce the level of GAGs. In wash-out group, the total amount of GAGs (0.93 ± 0.40 mg/g; $n = 4$; $p = 0.1734$) recovered to a level similar to the rehabilitating group, suggesting a partial return of GAGs (Fig. 2A). 4-MU and/or rehabilitative effect on GAGs level was tested against placebo group.

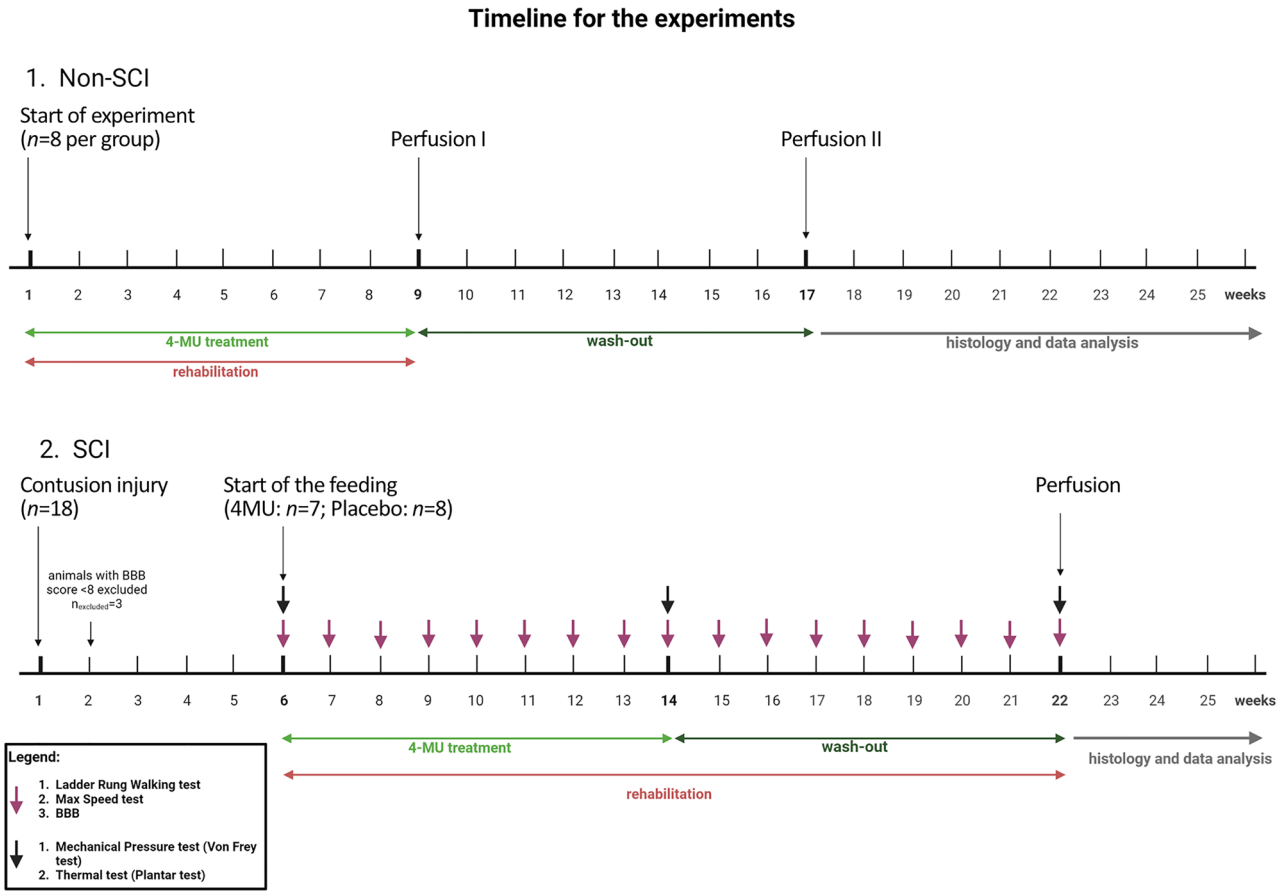

Figure 1. Schematic illustration of the experimental timeline. Created with BioRender.com.

We also quantified the level of HA down-regulation using HABP staining (Fig. 2B,C). Histochemical staining was performed on sections at Th6 and Th10 and around the Th8 level which is the focus of subsequent experiments. In 4-MU treated group, the intensity of HABP was significantly decreased at Th8 (74.32 ± 12.81; $n = 3$; $p < 0.0001$) and Th6 sections (68.68 ± 4.20; $n = 3$; $p = 0.0007$) when compared to placebo group (at Th8, 114.53 ± 6.36, $n = 3$ and at Th6, 114.57 ± 10.97, $n = 3$). There was no significant difference between 4-MU-treated and placebo groups at Th10 level. After 2 months of wash-out, HA remained at low levels at Th8 (79.37 ± 5.57; $n = 3$; $p = 0.0005$) and Th6 (83.24 ± 11.00; $n = 3$; $p = 0.0962$) compared to the placebo group, with some trend of return of HA production but not reaching the level of the placebo group (Fig. 2B,C).

Quantification of the mRNA expression of HASs in spinal cord samples using qPCR (Fig. 2D) revealed no significant down-regulation of *HAS genes* expression in the 4-MU group. However, clear trends of down-regulation were observed for *HAS genes* expression in 4-MU group when compared to all other groups. In the wash-out group, the *HAS genes* expression reached placebo levels combined with rehabilitation group, suggesting a recovery of normal GAGs expression after the wash-out period.

We next investigated the effect of 4-MU treatment (at a dose of 1.2 g/kg/day) on PNNs in the ventral horns by co-staining of WFA and ACAN. WFA is a widely used PNN marker and has been shown to specifically label the N-acetyl-D-galactosamine residue at terminal ends of chondroitin sulfate chains[32,33]. ACAN is a major PNN component and has been reported to be superior in labelling PNN positive motoneurons in the spinal cord[17]. Spinal cord sections from all 5 groups were stained for WFA (Fig. 3A, green arrows) and ACAN (Fig. 3A, red arrows), the number of positive cells in the ventral horns up to the central canal was counted (Fig. 3B–D). Similar to the biochemical assays, 4-MU treatment and treadmill exercise independently reduced the total number of WFA-positive cells in spinal ventral horns (Fig. 3B–D). The combination of both induced a stronger down-regulation, however, this did not reach significance. In addition, we also observed that the number of WFA and ACAN positive neurons returned to control levels after wash-out period. PNNs have been previously shown to enwrap α-motoneurons in the spinal cord. With the use of anti-ChAT antibody, we observed reduced PNNs around ChAT-positive neurons in thoracic uninjured spinal cords after 4-MU treatment (Fig. 3E). This suggests that the current 4-MU dose at 1.2 g/kg/day or rehabilitation can effectively reduce PNNs in the uninjured spinal cord.

4-MU (1.2 g/kg/day) is insufficient to down-regulate the increasing production of chondroitin sulfates after SCI

Having found that a 4-MU dose of 1.2 g/kg/day combined with rehabilitation could effectively reduce PNNs in the spinal cord, we next investigated whether this dose is sufficient to reduce the increased expression of inhibitory

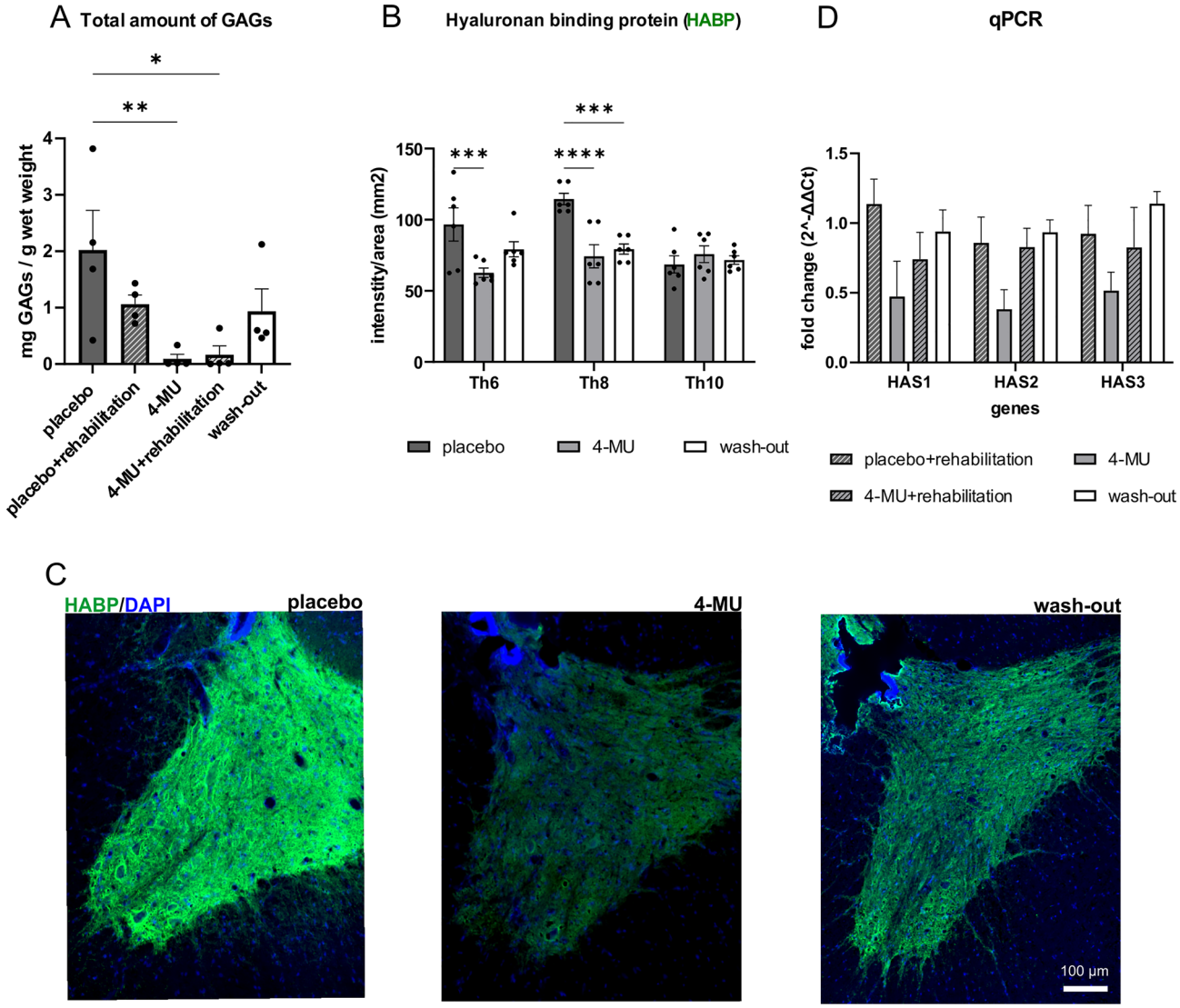

Figure 2. 4-MU decreases hyaluronan (HA) and chondroitin sulfate proteoglycans (CSPGs) synthesis in non-SCI animals. (**A**) Bar graph showing the total amount of glycosaminoglycans (GAGs) extracted from frozen spinal cords after 4-MU or placebo feeding, and wash-out period. Values are plotted as mean ± SEM; * $p < 0.05$, by one-way ANOVA, Dunnett's *post-hoc* test. ($n = 4$ animals per group). (**B**) Quantification of (C). Bar graph shows the mean intensity per area of grey matter together with the individual data points. Intensity was calculated using the HistoQuest software from TissueGnostics. Values are plotted as mean ± SEM; * $p < 0.05$, ** $p < 0.01$ by two-way ANOVA, Dunnett's *post-hoc* test. ($n = 3$ animals per group, 2 images per animal). (**C**) Representative fluorescent images showing different hyaluronan binding protein positive (HABP +) signal intensity in gray matter (Th8) in placebo, 4-MU treated and wash-out group after 8 weeks of feeding and after 2 months of wash-out period. Scale bar 100 µm. (**D**) Bar graph shows fold changes of the expression of *hyaluronan synthase* (*HAS*) *1, 2, 3* genes (as 2^-ΔΔCt), normalised to the placebo treated animals without rehabilitation. 2^-ΔΔCt values were determined by qRT-PCR. Values are plotted as mean ± SEM; two-way ANOVA, Tukey *post-hoc* test in all 4 groups. ($n = 4$ animals per group).

ECM in injured spinal cord. Rats received 200 kdyn impact to the Th8 spinal level which induced moderate SCI. Six weeks after the injury, the animals were divided into two groups, and the groups were fed a daily diet containing 4-MU- or placebo for 8 weeks. In addition, both groups received task-specific rehabilitation for the 16 weeks concurrent to the oral 4-MU treatment (i.e. 8 weeks during 4-MU treatment and 8 weeks afterwards) in order to prime appropriate re-connection from the potentially heightened neuroplasticity (Fig. 1, SCI).

First, we evaluated the level of HA within the spinal cord (Fig. 4) using HABP. There is a significant reduction of HA surrounding the lesion, rostrally (up to 5 mm) and caudally (1 and 5 mm) from the lesion in the 4-MU-treated group (40.78 ± 6.30) compared to placebo group (72.46 ± 6.46). We observed the trend of lower level of HA throughout the spinal cord after 4-MU treatment. The intensity remained decreased even after 8 weeks of wash-out period.

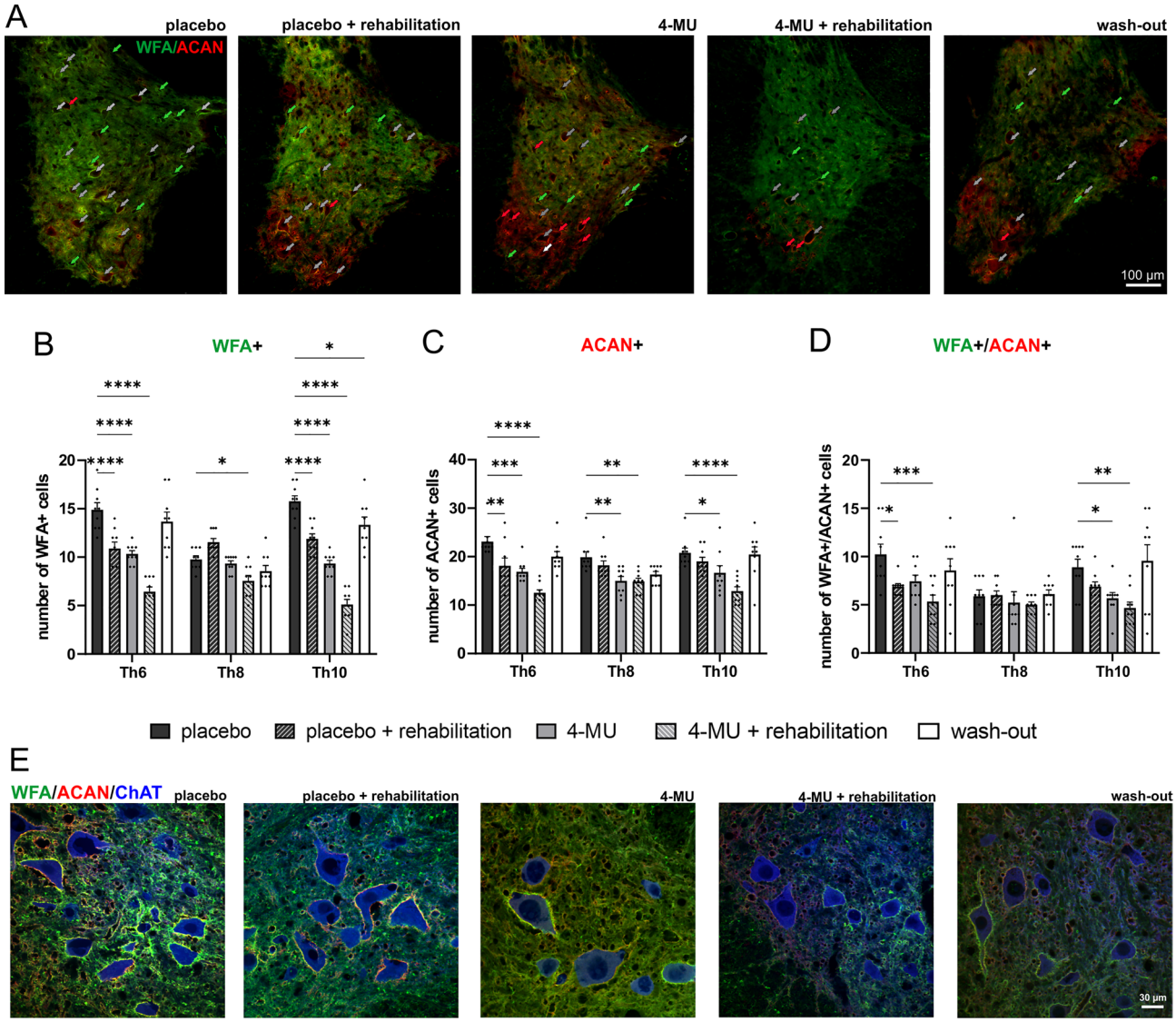

Figure 3. Down-regulation of perineuronal nets (PNNs) after 8 weeks of 4-methylumbelliferone (4-MU) feeding in uninjured animals, with or without daily treadmill training, and the re-appearance of perineuronal nets (PNNs) after 2 months of wash-out period. (**A**) Representative fluorescent images showing *Wisteria floribunda* agglutinin (WFA) and aggrecan (ACAN) positive PNNs around cells in the ventral horns and their colocalization (WFA + /ACAN +) in thoracic spinal cord (Th8) in uninjured animals in all 5 groups after 8 weeks of feeding and after 2 months of wash-out period. Green arrows indicated the WFA positive PNNs enwrapped cells; red arrows indicated ACAN positive PNNs enwrapped cells and gray arrows indicated cells where WFA/ACAN positive signal colocalizes. Scale bar 100 µm. (**B**–**D**) Quantitative analysis of WFA positive or ACAN positive PNNs. Data showed mean ± SEM ($n = 3$ animals per groups, 3 sections per animal). *$p < 0.05$, **$p < 0.01$, ***$p < 0.001$, ****$p < 0.0001$, two-way ANOVA, Dunnett's multiple comparison. (**E**) Representative confocal images showing WFA positive and ACAN positive PNNs surrounding ChAT positive motoneurons in the thoracic rat spinal cord (Th8) in placebo, 4-MU treated and wash-out group in ventral horn. Scale bar 30 µm.

We then evaluated the level of PNNs and CSPGs using WFA and ACAN. Our results showed no significant difference between 4-MU-treated and placebo groups for 8 more weeks without any treatment but daily rehabilitation (Fig. 5). These findings correspond with our data from uninjured animals where PNNs re-appeared after 2 months wash-out period (Figs. 1 and 2). The strong up-regulation of CSPGs after SCI has rendered the dose of 1.2 g/kg/day 4-MU to be insufficient to supress their production in injured spinal cord.

4-MU reduces glial scar in chronic spinal cord injury

HA is produced by both neurons and glia in the CNS, and is up-regulated by astrocytes in neuroinflammation[34–36]. It has been previously suggested that 4-MU reduces astrogliosis in the brain parenchyma in the mouse model of the experimental autoimmune encephalomyelitis[37]. In view of our observation in HA down-regulation around the lesion cavity, we next focused on the effect of 4-MU to the glial scar after SCI. Quantitative analysis of

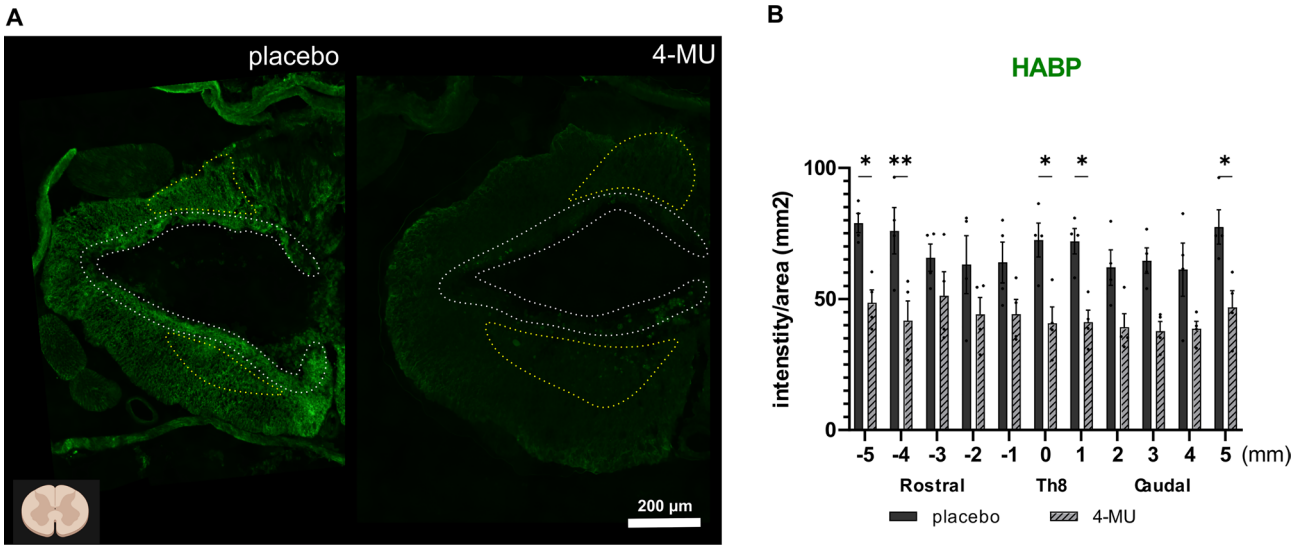

Figure 4. Hyaluronan binding protein (HABP) intensity remained decreased following chronic spinal cord injury, 8 weeks of 4-MU treatment and 8 weeks wash-out period combined with daily rehabilitation. (**A**) Representative fluorescent images showing different HABP positive signal intensity in spinal cord injured (SCI) rats in placebo and 4-MU-treated groups after 8 weeks of feeding and after 8 weeks of wash-out period. Bar graph shows the intensity per sections throughout the spinal cord. White dotted lines delineating the border of the cavity. Yellow dotted lines depicting the spared gray matter. The area of the spared gray matter differs among animals due to injury variability and individual character of the animals. 3 animals were excluded based on BBB test 1 week after the injury (i.e., animals with less-than 8 score in BBB test were not included in the present study). Diagram in the bottom left shows the orientation of the cross sections, created with BioRender.com. Scale bar 200 µm; (**B**) Quantification of (A). Individual data together with their mean ± SEM were shown ($n = 3$ animals per group). *$p < 0.05$, **$p < 0.01$, by two-way ANOVA, Sidak's multiple comparisons test.

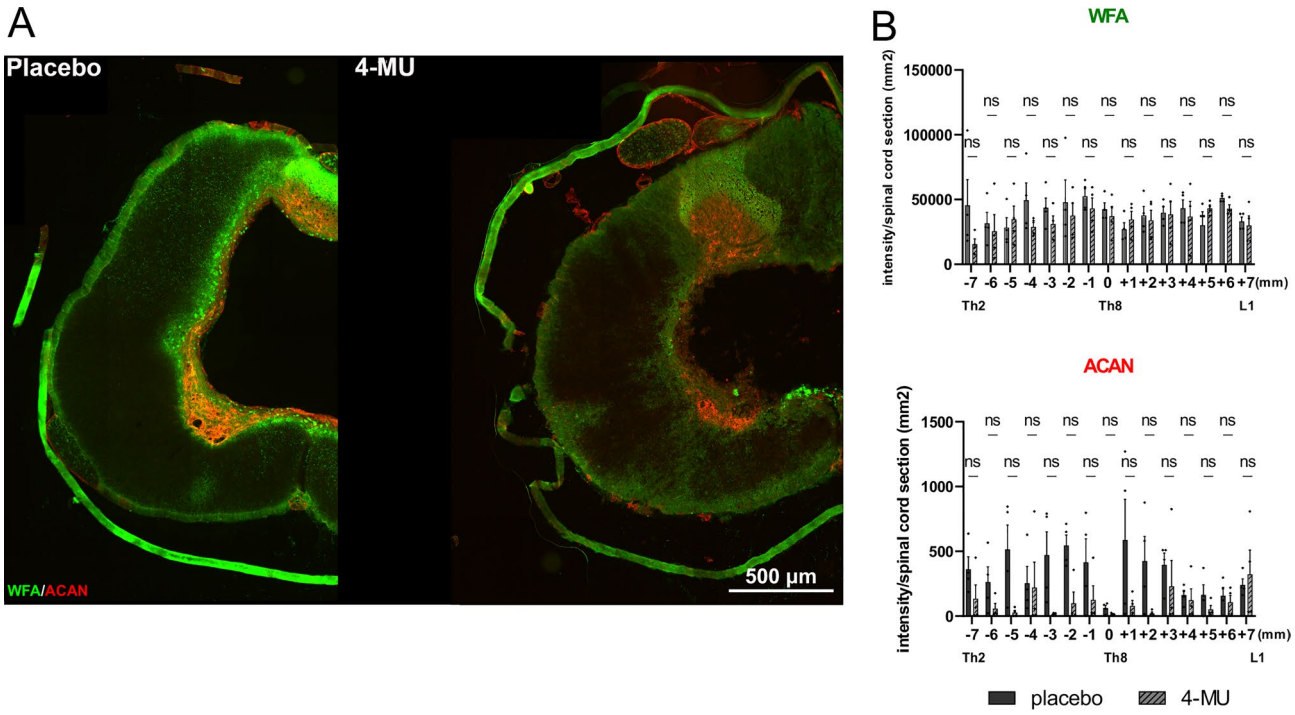

Figure 5. Immunofluorescence double-staining of *Wisteria floribunda* agglutinin (WFA) and aggrecan (ACAN) suggested that 4-MU at current dose 1.2 g/kg/day is not sufficient to down-regulate the increasing production of chondroitin sulfates after spinal cord injury (SCI). (**A**) Representative fluorescent images showing WFA positive (in green) and ACAN positive (in red) area around the centre of the lesion. Scale bar 500 µm; (**B**) the quantitative analysis of WFA or ACAN intensity. Bar graphs show the intensity per sections throughout the spinal cord with the lesion centre marked as level 0. Individual data points and their mean ± SEM were shown ($n = 4$ animals per group). ns by two-way ANOVA, Sidak's multiple comparisons test.

GFAP-positive area was performed to assess the glial scar surrounding the lesion cavity on cross sections (Fig. 6). A significant decrease in astrogliosis was observed in 4-MU treated group at a dose of 1.2 g/kg/day compared to placebo group. The average peak in the centre of the lesion in 4-MU groups was 1.49 ± 0.51% ($n = 4$) and 6.1 ± 1.94% ($n = 4$) in placebo groups (Fig. 6C). It is also noted that the GFAP staining at the periphery of the 4-MU sections seem to be brighter than the placebo control groups. We thus analysed the pixel intensity between the two groups and did not observe any significant difference.

To determine whether 4-MU affects only GFAP expression in scar-forming astrocytes or the astrocytes themselves, we performed immunohistochemistry for nestin and compared their behaviour to GFAP-positive cells around the lesion epicentre (Th8–Th9), below (Th10–Th11) and above (Th5–Th6) the lesion (Fig. 7F). Intensity measurement showed a reduction in signal for both nestin and GFAP after 4-MU treatment, when compared to placebo. This suggests that there is a reduction in astrocyte proliferation and activation.

We next checked how 4-MU treatment affects microglia/macrophages and oligodendrocyte progenitor cells (OPCs). We used the ionised calcium-binding adaptor molecule 1 (Iba-1) as a microglia/macrophage-specific calcium-binding protein (Fig. 7B,F). We observed a significantly higher number of Iba-1 positive cells at the lesion site after 4-MU when compared to the placebo group. This suggests that 4-MU mediates the infiltration of microglia and macrophages in the area.

Next, we examined the changes in OPCs using neuron-glial antigen 2 (NG2) and observed a significant increase in NG2 signal after long-term treatment with 4-MU followed by a 2-month washout period (Fig. 7C,F). As NG2-expressing OPCs can either be (i) contributing to scar-formation in response to the secretion of bone morphogenic protein (BMP) by the activated astrocytes or (ii) self-renewal and facilitates regeneration, further experiments will be required to confirm their functions at the lesion area. Nonetheless, these results demonstrated that 4-MU treatment is modulating the cellular composition around the lesion area.

To investigate the changes in the extracellular matrix around the lesioned area, we have examined the level of CSPGs and collagen 1a (Fig. 7D–F). With the use of CS-56 antibody which recognises CS-GAG chains, we observed a significantly down-regulation of CS-56 signal at the lesion epicentre in the 4-MU treated group when compared to the placebo group. This is in contrast to the WFA and aggrecan staining in Fig. 5 where no significant change was observed. As CS-56 is specific for chondroitin sulfate types A and C enriched sequence[38], our results suggests that there is a differential regulation in sulfation pattern around the lesion site after 4-MU treatment. The mechanism of how 4-MU induces such changes is unclear.

We then examined the levels of collagen 1a which is produced by meninges or fibroblasts. There was no significant change in the presence of collagen 1a-positive cells at the lesion site or away from the lesion.

Daily 4-MU at a dose of 1.2 g/kg/day promotes sprouting of serotonergic fibres distant from the injury but has no effect on synaptic density around the lesion site

4-MU has previously been shown to down-regulate PNNs in the brain at a dose of 2.4 g/kg/day[24]. The results in Figs. 4, 5, 6 and 7 showed that while lower dose of 1.2 g/kg/day is able to reduce HA and glial scar, the level of CSPGs remains similar to untreated injured controls after SCI (Fig. 5), and that there are sulfation modifications on the CS-GAG chains. Serotonin (5-hydroxytryptamine; 5- HT) is an important neurotransmitter in the mammalian spinal cord that plays an essential role in controlling sensorimotor functions. We thus investigated if 4-MU treatment leads to any changes in serotonergic innervation. We observed that after an 8-week treatment with 4- MU and a 2-month washout period plus rehabilitation, there was a significant increase in 5-HT positive puncta in the ventral horns above the lesion in the 4- MU treated group (259.25 ± 12.3) compared to the placebo group (208.58 ± 4.06), and below the lesion in the 4-MU treated group (270.67 ± 15.17) compared to the placebo group (203.96 ± 6.01) (Fig. 8A,B). The results suggest that 4-MU treatment, in combination of rehabilitation during the 8-week washout period, leads to the downregulation of HA and promotes long-term synaptic plasticity after chronic spinal cord injury.

To investigate whether there is a difference in overall synaptic density (Fig. 8C,D), we stained 2 levels above and below the lesion for the presynaptic marker synapsin and measured the level of synaptic contacts within ventral horns. 4-MU treated animals showed a trend of increased synaptic density in the area above lesion, but with no significant difference (Fig. 8D). There is no change in synaptic density measurement below lesion, probably due to the lack of CS reduction as observed in Fig. 5.

4-MU at a dose of 1.2 g/kg/day is not sufficient to enhance inherent functional recovery in chronic stage of spinal cord injury

On account of biochemical results showing that 4-MU abolishes plasticity-limiting perineuronal nets, we tested if the axonal sprouting induced by 4-MU and daily rehabilitation would lead to functional recovery in chronic stage of SCI. To test this, the whole battery of behavioral tests was performed, including weekly BBB test, maximum speed test and ladder rung walking test combined with daily rehabilitation on treadmill assessing their locomotor abilities. Two sensory tests, mechanical pressure test (Von Frey test) and thermal test (Plantar test) were chosen to assess changes in thermal and mechanical sensation. These two tests were performed trice—before feeding with 4-MU-containing/placebo pellets, at the end of feeding period, and at the end of the whole experiment. In our results, there were no significant differences or indication for a trend of improvement at any time point suggesting the lack of 4-MU-mediated recovery (Fig. 9).

Discussion

We investigated whether a dose (1.2 g/kg/day) of 4-MU was sufficient to decrease PNNs in ventral horns, and to promote sprouting and functional recovery in chronic SCI. Previous study in mice using 2.4 g/kg/day has led to an enhancement neuroplasticity for memory acquisition through PNN down-regulation[24]. As the LD_{50} is slightly

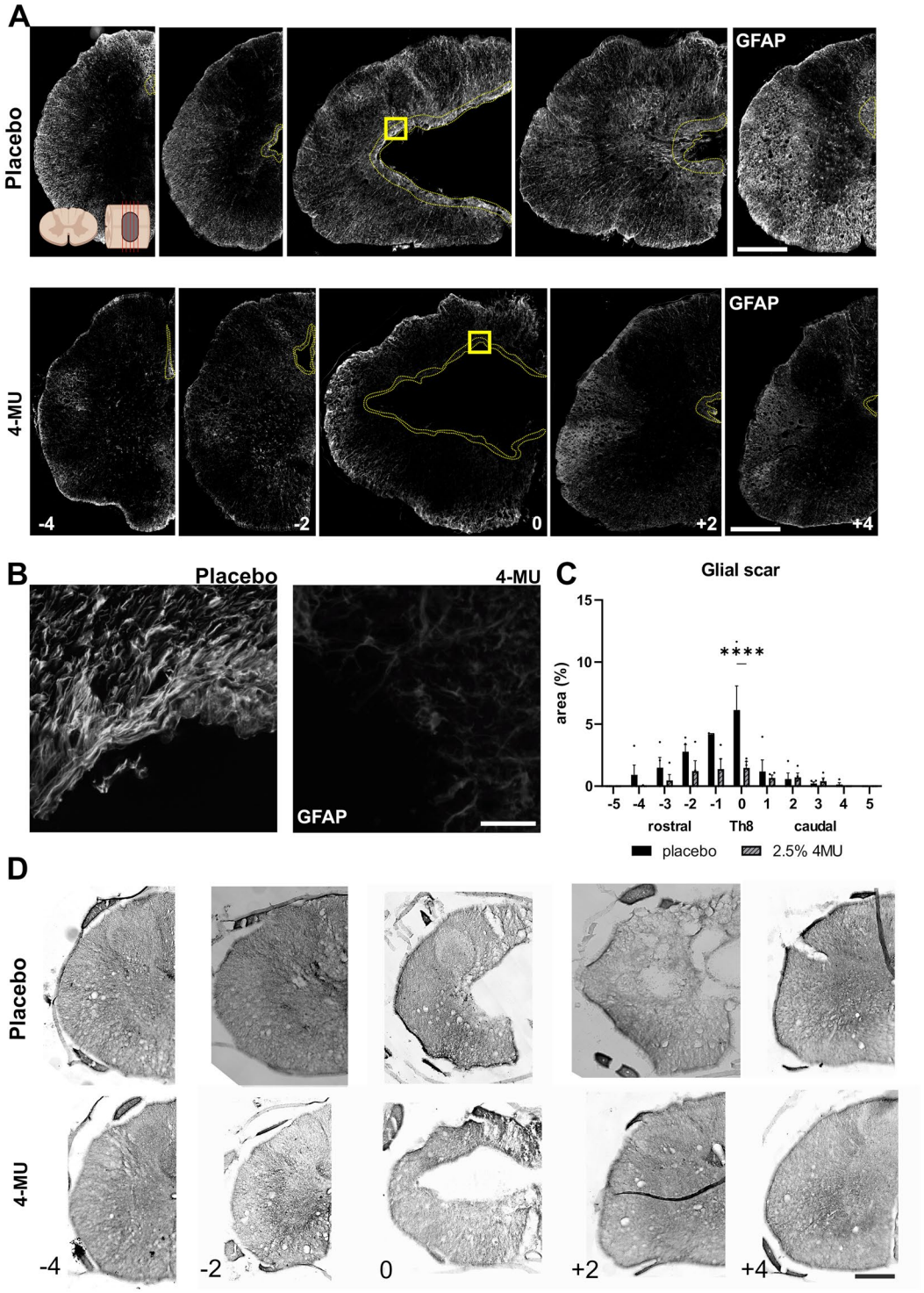

Figure 6. 4-MU treatment reduced glial scar area surrounding the lesion site. (**A**) Representative fluorescent images showing lesion epicentre (0 mm), above (− 4, − 2 mm) and below (+ 2, + 4 mm) the lesion, stained for glial fibrillary acidic protein (GFAP) in placebo and 4-MU treated group with chronic spinal cord injury. Dotted lines show the border area of the lesion cavity in 4-MU treated group and GFAP positive area in placebo group. Scale bar: 200 µm. Diagram of uninjured spinal cord at top left showing the direction of the cross section in (**A**), created with BioRender.com; (**B**) magnified images (yellow square in **A**) showing structural change of the glial scar tissue after 4-MU treatment compared to placebo treated animals. Scale bar 30 µm; (**C**) bar graph showing area of the glial scar around the central cavity performed in the GFAP stained histochemical images using ImageJ software. Values are plotted as mean ± SEM; $^{****}p < 0.0001$ by two-way ANOVA, Sidak *post-hoc* test. ($n = 4$ animals per group). (**D**) Representative images of Luxol Fast Blue staining showing the lesion extension in a rostro-caudal direction. Scale bar 200 µm.

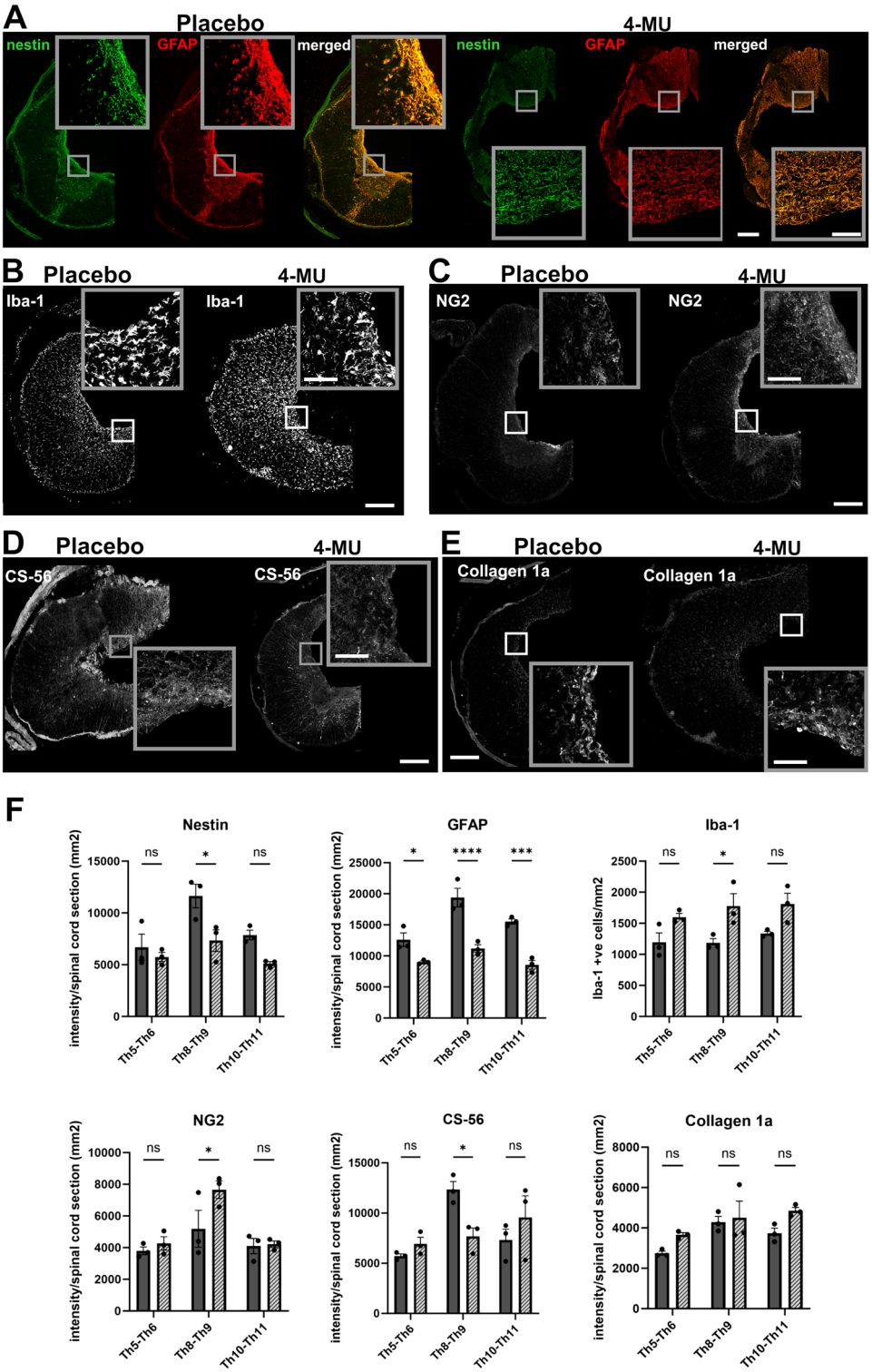

Figure 7. 4-MU treatment leads to changes of cell and ECM composition around the lesion scar (Th8-9), above (Th5-6) and below (Th10-11) lesion. (**A**–**E**) Representative confocal images showing the 4-MU-mediated effect on scar-forming cells and components using different markers—(**A**) nestin and GFAP were used to visualise scar-forming astrocytes. (**B**) Iba-1 to visualise microglia/macrophages. (**C**) NG2 to visualise oligodendrocyte progenitor cells (OPCs). (**D**) CS-56 to examine the changes in CS sulfations. (**E**) Collagen 1a to visualise meninges and fibroblasts. All insets show magnified views of the staining. Scale bar 200 µm for the overview image and 50 µm for the insets. (**F**) Quantification of (**A**–**E**). Bar graphs show intensities per section throughout the spinal cord, except for Iba-1 staining where the number of Iba-1 positive cells per mm was counted. Individual data are shown with their mean ± SEM (n = 3 animals per group). $p < 0.05$, $^{**}p < 0.01$, $^{***}p < 0.001$, $^{****}p < 0.0001$, by two-way ANOVA, Sidak's multiple comparison test.

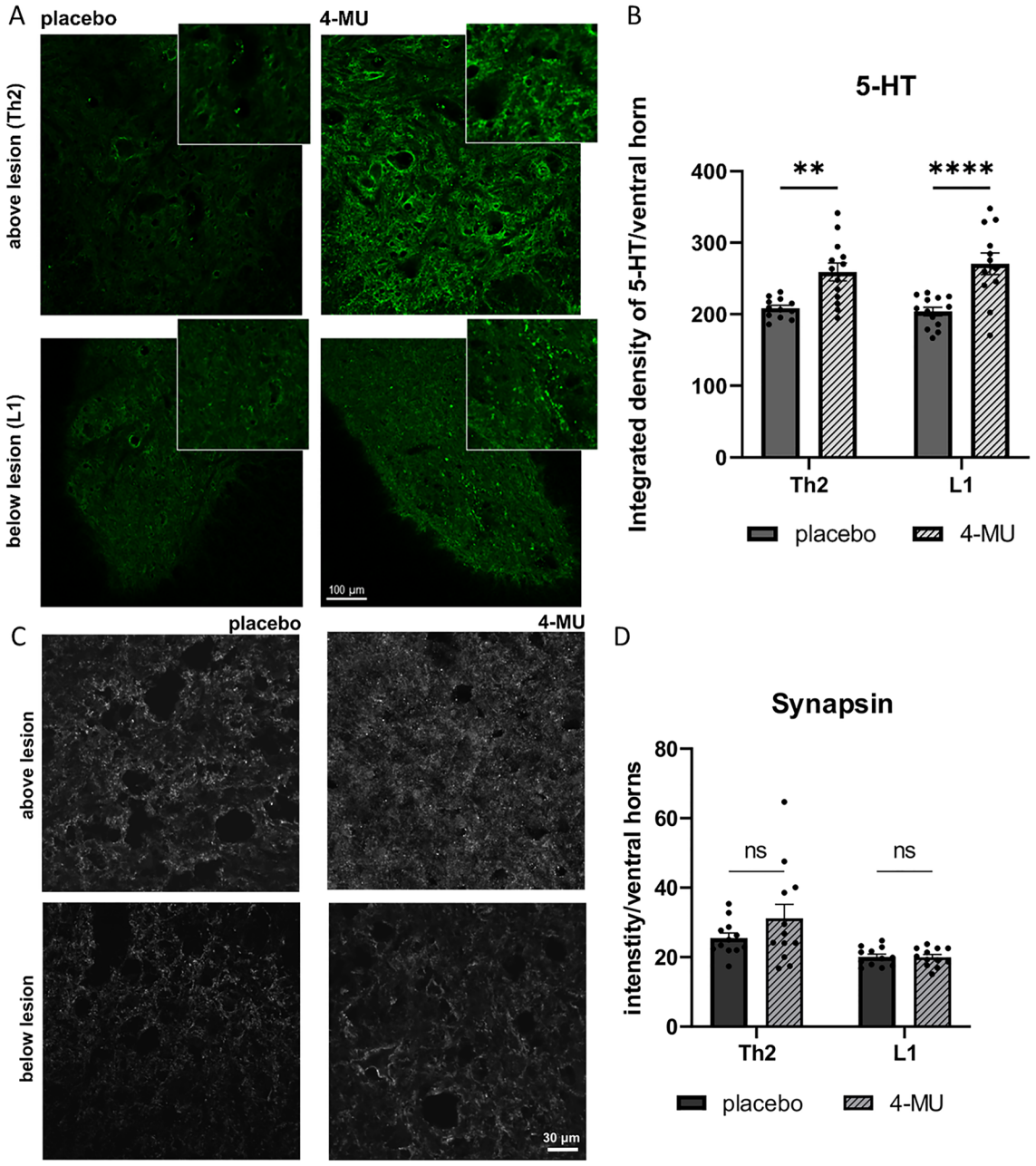

Figure 8. 4-MU treatment increases the puncta of serotonergic fibre distant from the lesion but does not increase synapse number at the lesion site after chronic spinal cord injury (SCI). (**A**) Representative confocal images showing ventral horn above and below lesion stained for 5-hydroxytryptamine (5-HT) in placebo and 4-MU treated group in chronic stage of SCI. Insets show the magnified views of the staining. Scale bar 100 µm; (**B**) bar graph showing the integrated density of 5-HT positive signal in ventral horns using ImageJ™ software. Values are plotted as mean ± SEM ($n = 4$ animals per group; 2–3 sections per animal); $^{**}p < 0.01$, $^{****}p < 0.0001$ by two-way ANOVA, Sidak's multiple comparisons test. (**C**) Representative confocal detailed images showing ventral horn above and below lesion stained for synapsin in 4-MU treated and placebo group in chronic stage of spinal cord injury. Scale bar 30 µm; (**D**) Bar graph showing intensity measurement per area (in pixels) of ventral horns using ImageJ software. Values are plotted as mean ± SEM ($n = 4$ animals per group; 3 sections per animal); ns > 0.05 by two-way ANOVA, Sidak's multiple comparisons test.

lower in rats than in mice, we therefore tested whether reducing this dose to half, i.e., 1.2 g/kg/day, would be able to down-regulate PNNs for possible functional recovery after SCI in rats. We found that the orally administered dose of 1.2 g/kg/day (4-MU) was sufficient to reduce PNNs and HA in uninjured animals, however, this is not sufficient to suppress the strong CSPGs upregulation after SCI, so that functional recovery was not observed.

In recent years, many studies have shown strategies focusing on regeneration after SCI, often based on targeting PNNs and manipulating the glial scar to attenuate inhibitory properties of its environment. Current strategies

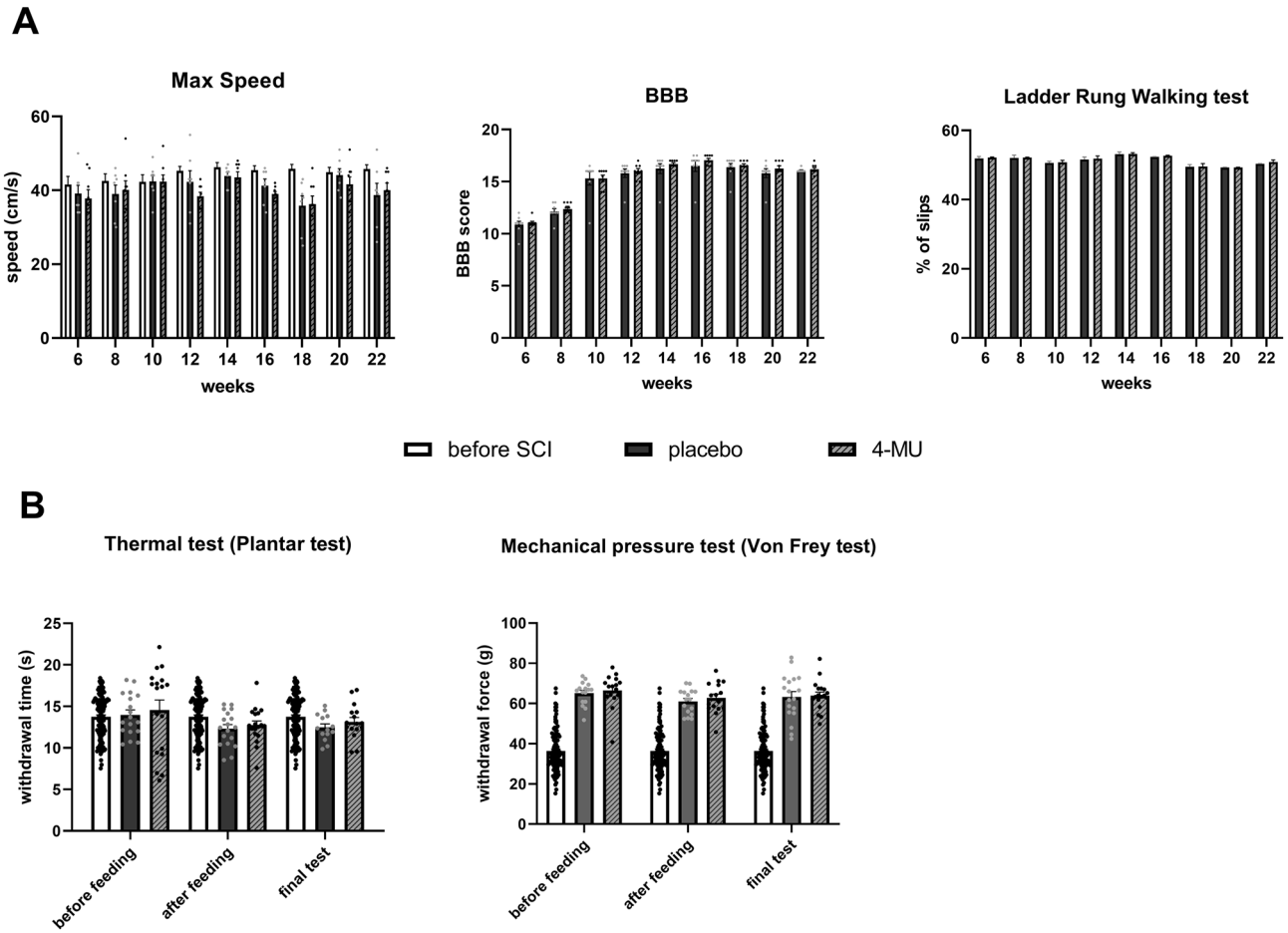

Figure 9. 4-MU treatment at a current dose does not lead to functional recovery after chronic SCI. The animals were tested weekly for their ability to reach the highest possible speed on the treadmill (max speed), to move around in open-field test (Basso, Beattie, Bresnahan—BBB), dexterity (ladder rung walking test), and sensory functions (Plantar and von Frey tests) at the three different time points of the experiment. (**A**) The bar graphs show the results of the behavioural tests assessing locomotion in rats—maximum speed (max speed), BBB, ladder rung walking test. The data show spontaneous recovery in both groups after the first two weeks of daily rehabilitation in the BBB Open Field Test, which stagnated in both groups at week 10. There was no 4-MU-mediated enhancement of this spontaneous recovery. Values are presented as mean ± SEM ($n = 7$ animals for the placebo group and $n = 8$ animals for the 4 MU group); ns > 0.05 by two-way ANOVA, Sidak's multiple comparison test (BBB, ladder rung walking test); ns > 0.05 by two-way ANOVA, Tukey's multiple comparison test (max speed). (**B**) The bar graphs show sensory function scores—before and after feeding and at the end of the experiment. No significant difference was found. Values are presented as mean ± SEM ($n = 7$ animals for the placebo group and $n = 8$ animals for the 4-MU group); ns > 0.05 by two-way ANOVA, Tukey's multiple comparison test.

range from proteolytic ECM manipulation to targeting the specific ECM components through the synthesis of inhibitory ECM molecules after SCI[39]. One of the most studied approaches has been an enzymatic ECM modification using ChABC. ChABC degrades CS chains into disaccharides and removes CSPG inhibition in the glial scar as well as removes the PNNs as plasticity brake, to benefit both acute and chronic SCI conditions[40]. Animals with SCI show better recovery both anatomically and functionally after ChABC treatment[19,20,40]. Functional recovery after SCI is further boosted when plasticity restoration is combined with rehabilitation[20,40]. However, ChABC application has several disadvantages. The major disadvantage of using this bacterial enzyme is its thermal instability and short half-life, which requires multiple or continuous intrathecal administrations[41], potential immune response of the body and difficult dosing. Apart from ChABC, Keough and colleagues[1] were testing a subset of 245 drugs known for their CNS penetrating capacity and oral bioavailability. None of these 245 compounds showed sufficient ability to overcome CSPG inhibition from oligodendrocyte precursor cells.

4-MU, the derivative of coumarin, used for biliary stasis therapy, is a HA inhibitor[25]. It has been previously shown to reduce the synthesis of HA by decreasing the production of UDP-GlcA, a key monosaccharide substrate for the synthesis of HA[42], and the expression of HASs. As UDP-GlcA is also a substrate for CS production, we thus investigate if 4-MU administration would decrease the synthesis of both HA and CS, facilitating neuroplasticity. Indeed, we have observed the down-regulation of HA and CS, both anatomically using histochemistry and biochemically through GAG quantification (Fig. 2). Our data suggest that 4-MU combined with daily training

suppresses the synthesis of GAG. With the use of PNN markers including WFA and ACAN, 4-MU administration led to PNNs removal in ventral horns. PNNs re-appeared after 2 months of wash-out period. The reason why PNNs reappeared while the HA level remained low after 2 months of wash-out is likely because CS synthesis is less sensitive to the UDP-GlcA deficiency. CS is synthesized in the Golgi apparatus where UDP-GlcA sugars are being transported to the Golgi lumen with high affinity, while HA is synthesized directly at the cytoplasmic membrane[25].

We used a thoracic contusion injury that spares some axons around a central cavity and ablates dorsal corticospinal tracts (CSTs) critical for motor control in humans, thus mimics the type of closed SCI most commonly seen in humans[43]. The 4-MU treatment started in the chronic stage, *i.e.* 6 weeks after the injury[44]. At this stage, glial scar is well-established, CSPGs are upregulated, and the acute immune response had already subsided[45,46]. 4-MU treatment was accompanied by daily rehabilitation on treadmill to consolidate appropriate synaptic connections and prune away others[47]. After the 8 weeks of treatment and rehabilitation, rehabilitation was continued for another 8 weeks for the wash-out. This wash-out period gives time for PNNs to re-form and stabilize de novo synapses and consolidate anatomical plasticity[20,22,40], while the continuing rehabilitation prunes random connections, supporting appropriate connections and removing inappropriate ones[48,49]. Oral administration of 1.2 g/kg/day 4-MU robustly decreased the glial scar surrounding the cavity that persisted throughout the wash-out period.

To evaluate the potential of 4-MU to remove the plasticity brake formed by PNNs, we analysed the intensity of 5-HT signal and observed increased 5-HT sprouting distant from the lesion. However, this sprouting did not lead to any significant difference in synapsin immunoreactivity within the ventral horns, above and below the lesion, between the 4-MU-treated and placebo animals. We also investigated the effect of 4-MU in mediating changes in other cellular composition. Indeed, we observed a reduction in both GFAP and nestin staining suggesting a reduction in astrogliosis. In addition, we observed an upregulation of Iba-1 and NG2 staining, suggesting mobilisation of microglial/macrophages and OPC into the area. It is not yet clear at this stage if their mobilisation is resulting from a direct effect of 4-MU treatment or the modulation of ECM resulting from 4-MU. Nonetheless, this suggests that 4-MU is modulating immune cell population in the lesioned environment. Assessment of functional recovery using the BBB test, maximum speed test and ladder rung walking test yielded no significant differences between the 4-MU and placebo treated groups, even with the continuous rehabilitation for next 2 months. As 4-MU-mediated PNNs ablation has been already demonstrated in previous work focused on mouse hippocampus where it enhances memory in ageing mice[24], we reasoned that the lack of functional recovery after SCI in this study is due to the lower dose of 4-MU administered (1.2 g/kg/day *versus* 2.4 g/kg/day) and the strong CS-GAG upregulation after injury. A higher dose of 4-MU combined with rehabilitation should be tried for its effect on recovery after SCI.

The promising results we observed in the 5-HT staining are consistent with the published data. Previous studies have already shown that severe SCI paralysis is caused not only by a loss of direct muscle innervation by spinal motor neurons, but also by a loss in the supraspinal pathways involved in voluntary initiation of movements and by a loss in the descending pathways that supply motor neurons with neuromodulators such as 5-HT[50,51]. In the intact spinal cord, serotonergic innervation emanates almost entirely from the raphe nuclei in the brainstem, which are lost[52,53] or severely disrupted[54] after SCI. The drastic and abrupt decrease in serotonin availability below the lesion results in spinal networks that are no longer excitable or responsive[55,56], contributing substantially to SCI -induced paralysis[53]. Barzilay and colleagues have also shown that HA is involved in the propagation of serotonergic fibres thereby improving neuroplasticity[57]. 5-HT stimulates spinal interneurons and motoneurons, allowing appropriate muscle contraction[50,58]. In acute SCI, spinal motoneurons and interneurons lack 5-HT[59,60] resulting in paralysis and spinal shock[61,62]. Therefore, in chronic SCI, motor neurons partially recover their excitability despite the continued absence of 5-HT[63]. It has also been suggested that this compensatory mechanism requires activity-dependent tuning to contribute to motor activity following SCI[52]. Our behavioural data have also shown spontaneous recovery of locomotor activity in rats with the contusion model of SCI. This spontaneous recovery is not only important in animals, but also in human patients with incomplete SCI. In incomplete SCI, part of the descending connection to the brain is spared, so animals, as well as human patients, can learn to use these spared connections to achieve substantial recovery of walking function, especially through rehabilitative training[64–66]. Understanding and promoting this plasticity in spared connections is therefore an important focus of spinal cord research. For example, it is already known that spared corticospinal axons sprout above the injury and form new connections, including transmission of descending inputs around the injury through spared propriospinal pathways[67–69]. In addition, spared descending fibres sprout below the injury, a process that has been well correlated with recovery in animal models[66]. For these spared and new connections to be functional, neurons downstream of the injury must be ready to respond to these enhanced or restored descending signals. This probably requires compensation for the loss of neuromodulatory (5-HT) innervation. In vitro time-lapse imaging studies have shown that serotonergic growth cones are more active than cortical growth cones when challenged with CSPG, and that serotonergic neurons recover better after enzymatic digestion with ChABC[70]. These results suggest that 4-MU may cause serotonergic fibres to respond better to treatment in vivo as well, through its effect on CSPG expression. In the case of ChABC, the studies have shown that this could be at least partly due to differences in the cytoskeleton or receptors. We speculate that systemic administration of 4-MU together with overall rehabilitation on treadmill induced 5-HT sprouting in the spinal cord even though CSPGs were not downregulated around the lesion. The robust response of serotonergic neurons may also be related to increased expression of GAP-43, which is associated with axon growth or regeneration and is normally downregulated in adulthood[71,72]. Serotonergic neurons require GAP -43 postnatally for proper terminal arborisation, at least in the forebrain[73]. Moreover, serotonergic neurons also produce GAP -43 mRNA in adulthood[74], possibly increasing the sensitivity of 5-HT fibres to injury.

In order to determine if there is any compensatory mechanism for the loss of HA synthesis, we have evaluated the changes in mRNA expression for genes related to the HA synthesis (*Has1*, *Has2*, *Has3*)[25] (Fig. 2D). We did

not observe any significant difference despite the clear trend of down-regulation in their mRNA levels. The *has* genes expression after 1 mM 4-MU treatment, studied on human aortic smooth muscle cells showed reduction mainly in *Has1* and *Has2* transcripts after 4-MU treatment[75]. To determine the biochemical effect of 4-MU at 1.2 g/kg/day on the HA synthesis in uninjured animals, we used histochemical staining for recombinant HABP derived from human versican G1 domain which binds specifically to hyaluronan and does not bind to other glycosaminoglycans (Amsbio; data sheet). We observed that after 2 months of wash-out period, the level of HA remains decreased compared to healthy animals. This may pose a question of whether the HA down-regulation after 2 months of wash-out period may induce adverse effects after treatment.

Clinical trials with 4-MU (drug approved in Europe and Asia as hymecromone) showed excellent safety parameters during long-term administration of approved doses—1.2–3.6 g/day[76–82]. The longest reported duration of oral 4-MU administration was for 3 months in human patients[80] which is much shorter time according to correlation between age of laboratory rats and humans[83] and it might be taken into consideration while explaining these results as the safety profile of long-term 4-MU treatment is not fully established yet[25]. However, our recent study in healthy rats showed that long term oral application of 4-MU at a dose of 1.2 g/kg/day did not result in any serious adverse effects. When deviations from reference levels occurred, they normalised after a 9-week wash-out period in Wistar rats. Our results suggest that 4MU at a dose of 1.2 g/kg/day is suitable for long-term treatment[30].

In conclusion, this study demonstrates that oral administration of 1.2 g/kg/day of 4-MU reduces the total amount of GAGs, reduces glial scar and increases 5-HT puncta in chronic stage of SCI. However, these structural changes do not result in increased synaptic connections and are insufficient to induce functional recovery even after intensive rehabilitation. A higher dose of 4-MU is likely to be necessary to induce the functional recovery supported by synaptic plasticity.

Methods

All methods were performed in accordance with the relevant guidelines and regulations. All procedures on animals were approved by the ethical committee of the Institute of Experimental medicine of Academy of Science of the Czech Republic (ASCR) and performed in accordance with Law No. 77/2004 of the Czech Republic (Ethics approval number: 13/2020). Power calculation, based on previous studies, was performed prior to the experiment to estimate the number of animals needed. All work was performed according European Commission Directive 2010/63/EU, and the ARRIVE guidelines. Efforts were made to minimize pain and suffering.

Experimental animals

55 female Wistar RjHan:WI rats (8-week-old, 250–300 g; 2020–2021; CS 4105 Le Genest Saint Isle; Saint Berthevin Cedex 53941 France) were used in total. 40 animals were used for the histochemical and biochemical assessment of the 1.2 g/kg/day 4-MU dose effect in 4-MU-fed/non-fed combined with/without rehabilitation groups. This dose was chosen as we aim to test if a lower dose at 1.2 g/kg/day weight will be effective in reducing inhibitory ECM and at the same time, minimize the 4-MU consumption for potential adverse effects of long-term treatment for SCI[30]. These animals were divided into 5 groups (8 rats per group) using simple randomization—placebo, placebo + training/rehabilitation, 4-MU, 4-MU + rehabilitation, and 4-MU with planned 2 months post-feeding period (wash-out group). Based on our previous experiments, we are expecting an effect size of ≥ 1.7. A power calculation of $\alpha = 0.05$, number of groups = 5, a total sample size of 8 is required for each experimental group.

Hereafter, the histochemical and biochemical assessment of the treatment in uninjured animals was done, 18 animals underwent the spinal cord contusion, 3 animals with BBB score less than 8, one week after the injury were excluded. The feeding has begun 6 weeks after SCI when the chronic phase was fully established. Half of the animals received chocolate-flavoured chow containing 4-MU (1.2 g/kg/day) (treated group) and the second half just chocolate-flavoured chow without any treatment (placebo group). Placebo and treated groups received daily physical rehabilitation on treadmill. Feeding stopped after 8 weeks, but daily extensive rehabilitation continued for 2 more months.

Rats were housed by two in cages with 12 h light/dark with standard conditions (in temperature (22 ± 2 °C) and humidity (50% ± 5%)). Rats had free access to water and food ad libitum. All experiments were performed between 08:30 and 19:00 local time.

Animal surgeries

Animals received a moderate thoracic spinal cord contusion using a commercially available Infinite Horizon (IH) spinal cord injury device (IH-0400 Spinal Cord Impactor device; Precision Systems and Instrumentation, Lexington, KY, USA). Rats were anesthetized with 5% (v/v) isoflurane and maintained at 1.8–2.2% during the surgery, in 0.3 L/min oxygen and 0.6 L/min air. Animals were injected subcutaneously with buprenorphine (Vetergesic® Multidose, 0.2 mg/kg body weight). Using sterile procedures, a laminectomy was performed at the Th8/Th9 level with the vertebral column being stabilized with Adson tissue forceps at Th7 and Th10. The animals received 200 kilodynes (kdyn) moderate contusion injury. Manual expression of bladders was performed in the first two weeks after injury, and the rats were checked daily. Rats were given treatment of analgesics if signs of inflammation were observed. Animals were given a random number after the surgeries. The chow or the placebo was similarly given a random number, and fed to the animals according to the number. The experimenters were blinded to the treatment group during the behavioural analysis. The identity of the animals and their treatment group was revealed only after the evaluation.

At the end of the experiments, half of rats from each group was intraperitoneally anesthetized with a lethal dose of ketamine (100 mg/kg) and xylazine (20 mg/kg), perfused intracardially with 4% (w/v) paraformaldehyde

(PFA) in 1X-PBS and post-fixed in the same solution for 24 h. Spinal cords were dissected before storing in 30% (w/v) sucrose (Milipore, cat. no. 107651) in 1X PBS. The second half of the rats were sacrificed with a lethal dose of ketamine (100 mg/kg) and xylazine (20 mg/kg) before the spinal cords were dissected and froze on dry ice before storage at -80°C for subsequent qPCR and GAGs extraction. The anaesthesia used have previously been shown not to interfere with animal behaviour.

4-MU treatment

2.5% (w/w) 4-MU was mixed and prepared into rat chocolate-flavoured chow (Sniff GmbH, Germany). This percentage would allow the delivery of 4-MU at 1.2 g/kg/day to the rats when chow was consumed ad libitum, an amount assessed from our pilot experiment. Rats were fed with the 4-MU chow at 10 weeks of age (non-SCI cohort) or 6 weeks after the SCI (SCI-cohort). Rats were maintained on 4-MU diet for 8 weeks. The food intake was measured weekly to check for consumption (Fig. 1).

Histological and histochemical analysis

Two cm long spinal cords, with the Th8 level in the middle, were embedded in O.C.T. compound (VWR) and sectioned in frozen block of tissue before being sectioned into 40 µm thick slices for immunohistological analysis. The sections were made in series of 1 mm, compared to the anatomical atlas, and thus the spinal cord segments were identified.

40 µm sections (free-floating for uninjured spinal cords, and mounted on glass slides for injured spinal cords) were permeabilizated with 0.5% (v/v) Triton X-100 in 1X PBS for 20 min and then endogenous biotin was blocked using Avidin/Biotin blocking kit (Abcam; cat. no. ab64212) to reduce non-specific background. Tissue was then blocked in ChemiBLOCKER (1:10; Millipore cat. no. 2170), 0.3 M glycine, 0.2% (v/v) Triton X-100 in 1X PBS for 2 h. The sections were then incubated with labelling agents including biotinylated *Wisteria floribunda* agglutinin (1:150, 24 h), biotinylated hyaluronan binding protein (HABP) (1:150, 24 h) and/or primary antibodies: anti-choline acetyltransferase (ChAT)(1:600, 72 h); anti-ACAN (1:150, 24 h), anti-GFAP conjugated to Cy3 (1:800, 24 h), anti-5-HT (1:400; 24 h) or anti-synapsin (1:100; 48 h), anti-nestin (1:300, 48 h), anti-NG2 (1:300, 48 h), anti-GFAP (1:300, 48 h), anti-CS-56 (1:100, 24 h), anti-IBA1 (1:300, 48 h), and anti-collagen 1a (1:200, 48 h) as shown in Table 1. After washing, the sections were labelled with fluorescent-conjugated secondary antibodies (1:300; 2 h; room temperature (RT) (Table 1). Staining was imaged with a LEICA CTR 6500 microscope with FAXS 4.2.6245.1020 (TissueGnostics, Vienna, AT) software. Images were evaluated for the total number of cells in ventral horns with WFA-positive signal, ACAN-positive signal and number of co-localised cells using ImageJ™ (NIH, Bethesda, MD, USA). The HABP intensity was analysed with HistoQuest 4.0.4.0154 (TissueGnostics) software. 5-HT was imaged with confocal microscope Zeiss LSM 880 and synapsin images were taken with confocal microscope Olympus FV10i (Olympus Life Science, Waltham, MA, USA). The intensity of 5-HT and synapsin was measured in the ventral horn by ImageJ™ and compared between 4-MU-treated and placebo group. To quantify Iba-1-positive, the Analyse Particles function in the FIJI software was used (22,743,772).

1° Antibody/labelling agent	Epitope	Host	Company
Biotinylated *Wisteria floribunda* agglutinin (WFA)	Chondroitin sulfate in the PNNs	N/A	Sigma-Aldrich cat. no. L1516
Biotinylated hyaluronan binding protein (b-HABP)	Hyaluronan	N/A	Amsbio cat. no. AMS.HKD-BC41
Anti-ACAN	Aggrecan	Rabbit polyclonal	Sigma-Aldrich cat. no. AB1031
Anti-GFAP-Cy3	Glial fibrillary acidic protein	Mouse monoclonal IgG	Sigma-Aldrich cat. no. C9205
Anti-ChAT	Choline acetyltransferase	Mouse monoclonal IgG	Invitrogen cat. no. MA5-31383
Anti-5-HT	5-hydroxytryptamine	Mouse monoclonal IgG	Invitrogen cat. no. MA5-12111
Anti-synapsin	Synapsin	Rabbit polyclonal	Novus biologicals cat. no. NB300-104
Anti-Nestin	Nestin	Mouse monoclonal IgG1	Chemicon cat. no. MAB353
Anti-NG2	Neural/glial antigen 2	Rabbit polyclonal	Chemicon cat. no. AB5320
Glial fibrillary acidic protein	Glial fibrillary acidic protein	Chicken polyclonal	Abcam cat. no. ab4674
Anti-CS-56	Chondroitin Sulfate	Mouse monoclonal IgM	Sigma-Aldrich cat. no. C8035
Anti-IBA1	Ionized calcium-binding adapter molecule 1	Rabbit polyclonal	FUJIFILM Wako Pure Chemical Corporation cat. no. 019-19741
Anti- Collagen 1a	Collagen, type I	Mouse monoclonal IgG1	Abcam cat. no. ab6308
2° antibody/labelling agent	**Company**		
Streptavidin-Alexa fluor 488	Invitrogen cat. no. S32354		
Goat anti mouse Alexa fluor 488	Invitrogen cat. no. A11029		
Goat anti rabbit Alexa fluor 594	Invitrogen cat. no. A11012		
Goat anti mouse Alexa fluor 405	Invitrogen cat. no. A48255		
Goat anti mouse Alexa fluor 488	Invitrogen cat. no. A21042		
Goat anti rabbit Alexa fluor 594	Invitrogen cat. no. A11012		

Table 1. A table showing the primary antibodies and fluorescent-conjugated secondary antibodies used for the experiments.

For images where intensity was measured and compared, experimental conditions including for immunohistochemistry and microscopy were kept the same. The stained sections were imaged with the same laser power, gain and airy units.

Luxol Fast Blue (LFB) staining was used to visualise white and grey matter. LFB staining is used to identify myelin in nerve tissue. Spinal cord tissue was sectioned in 4 animals per group. A total of fifteen sections, including the centre of the lesion and both cranial and caudal areas, were observed and captured using a Zeiss LSM 880 Airyscan (Zeiss, Oberkochen, Germany).

GAGs extraction and analysis

Frozen tissues were first weighted before the incubation with acetone to remove the lipids. The samples were then dried and cut into small pieces before the pronase treatment (15 mg pronase per hemisphere, (Roche, cat. no. 11459643001) in 0.1 M Trizma hydrochloride (Sigma-Aldrich, cat. no. T3253), 10mM calcium acetate (Millipore, cat. no. 567418), pH 7.8. Samples were homogenized with Potter Elvehjem tissue homogenizer in the pronase solution. Residual protein fragments were precipitated with trichloroacetic acid (Sigma-Aldrich, cat. no. T6399). The supernatant, which contains the GAGs, was collected and stored on ice. The solution was then neutralised with 1 M Na_2CO_3 (Sigma-Aldrich, cat. no. S7795) to pH 7.0, and the GAGs were recovered by ethanol precipitation. The isolated GAGs were redissolved in 0.3 ml of deionised water. The GAG concentration was quantified using cetylpyridium chloride (CPC) turbidimetry. Standard curve was prepared from 1µg/µl of Chondroitin sulphate A (Sigma-Aldrich, cat. no. C9819)[31]. Briefly, the diluted sample was mixed with 0.2% (w/v) CPC and with 133 mM $MgCl_2$ (Sigma-Aldrich, cat. no. M2670) in ratio 1:1. Absorbance was measured at 405 nm using plate reader spectrophotometer (FLUOstar® Omega, BMG LABTECH). Each sample was carried out in three different dilutions and each dilution was carried out in duplicate.

Quantitative real-time polymerase chain reaction

For quantitative evaluation of gene transcript levels in spinal cords treated with or without 4-MU, quantitative real-time PCR (qPCR) was used. RNA was isolated with RNeasy© Lipid Tissue Mini Kit (QIAGEN, cat. no. 74804) according to the manufacturer's protocol. Amount of isolated RNA was quantified using NanoPhotometer© P330 (Implen, München, Germany). Then, TATAA GrandScript cDNA Synthesis Kit (TATAA Biocenter, Art No. AS103c) was used for reverse transcription of RNA into complementary DNA (cDNA), following the manufacturer's protocol in the T100TM Thermal Cycler (Bio-Rad, Hercules, CA, USA). For the qPCR, TaqMan® Gene Expression Assays (Life Technologies by Thermo Fisher Scientific, Waltham, MA, USA) were used for HAS1 (Rn01455687_g1), HAS2 (Rn00565774_m1), HAS3 (Rn01643950_m1) and GAPDH (Rn01775763_g1), all purchased from Applied Biosystems and used as recommended by the manufacturer. Amplification was performed on the qPCR cycler (QuantStudio™ 6 Flex Real-Time PCR System, Applied Biosystems® by Thermo Fischer Scientific, Waltham, MA, USA). All amplifications were run under the same cycling conditions: 2 min at 50 °C, 10 min at 95 °C, followed by 40 cycles of 15 s at 95 ◦C and 1 min at 60 ◦C. Expression was calculated using the threshold cycle (Ct) value and $\log(2^{-\Delta\Delta Ct})$ method and normalized to the control group. Each qPCR experiment was carried out in duplicate. Ct values of each measured condition were normalized to glyceraldehyde 3-phosphate dehydrogenase (GAPDH). Then, the $2^{-\Delta\Delta Ct}$ values were expressed as described by Livak and Schmittgen[84]. After that, the mean of each subset was calculated for each group.

Behavioural tests

Treadmill training

Treadmill training began 6 weeks after SCI and was conducted on 5 consecutive days per week for 16 weeks. The training consisted of 10 min run, 20 min break and 10 min run. The treadmill speed was 16–18 cm/s in the first and second weeks and 20 cm/s in the remaining weeks of training. Half of non-SCI rats were trained for 8 weeks as well, except wash-out group when the training had been prolonged for 2 months without 4-MU feeding.

Maximum speed test

Maximum Speed test was performed once per week and began 6 weeks after the SCI. The treadmill speed started at 20 cm/s and was increased every 10 s for 2 cm/s. When the animal was not able to run at a given speed, the treadmill was stopped and the last value was recorded.

Basso, Beattie and Bresnahan (BBB) test

The Basso, Beattie and Bresnahan (BBB)[85] open-field test was used to assess the locomotor ability of the rats. The rats were placed into the arena bordered with rectangular-shaped enclosing. The results were evaluated in the range of 0–21 point; from the complete lack of motor capability (0) to healthy rat-like locomotor ability (21). The measurements were performed 4th and 7th day after the SCI and then weekly for 8 weeks, starting 6 weeks after SCI.

Ladder rung walking test

For the advanced locomotor skills, the ladder rung walking test had been used. Animals were placed on a 1.2 m—long horizontal ladder, with irregularly spaced rungs. At the end of the ladder was a dark box that the rats favoured. The animals crossed the ladder 3 times in a row and all attempts were recorded on camera. The hind paws placement on the rungs was evaluated by using a seven-category scale (0–6 points), as previously described by Metz and Whishaw[86] from all three videos. Metz and Whishaw´s scoring scale was divided into 3 categories: 0–2; 3–4; 5–6. Videos were then evaluated and the percentage of steps in each of the 3 categories was calculated.

All the animals were pretrained before lesioning. The test was performed weekly for 16 weeks, starting 6 weeks after the SCI.

Mechanical pressure test (Von Frey test)
The Mechanical Pressure test was used to assess mechanical allodynia after the SCI and/or during treatment. The animals were placed in an enclosure with a metal mesh bottom and habituated there for 15 min. Von Frey rigid tip coupled with a force transducer (IITC Life Science, California, USA) was applied with a gradual increase of pressure to the footpad of the forepaw, until the animal withdrew its paw. The maximum pressure was recorded in grams. Five trials were performed on both hind paws. The trial was terminated if the animal failed to respond within 90 g. The average was set from three values after excluding the highest and lowest measurement. The test was performed 6 weeks after the SCI (before 4-MU treatment), after 8 weeks of rehabilitation (after 4-MU treatment), and at the end of the experiment.

Thermal test (plantar test)
The thermal test was used to assess a thermal hyperalgesia after the SCI and/or during treatment. The animals were placed in an acrylic box of the standard Ugo Basile test apparatus (Ugo Basile, Comerio, Italy) and habituated there for approximately 30 min. A mobile infrared-emitting lamp was then placed directly under the footpad of the hind paw, always in the same position. After placing the lamp, a thermal radiant stimulus was applied. The apparatus is connected to device what automatically recorded the time (in seconds) between the outset of the stimulus and the paw-withdrawal. Five trials were performed on both hind paws. The trial was terminated if the animal failed to respond within 30 s or wet oneself. The average was set from three values after excluding the highest and lowest measurement. The test was performed 6 weeks after the SCI (before feeding), after 8 weeks of rehabilitation (after feeding), and at the end of the experiment.

Statistical analysis
Data processing and statistical analysis were performed using GraphPad Prism (GraphPad Software). To analyse the effect of 4-MU treatment on chronic SCI in rats, different statistical tests were used. The two-way *ANOVA* followed by Sidak's multiple comparisons test was applied for astrogliosis, HABP, WFA, ACAN, 5-HT, synapsin intensity in SCI cohorts, BBB and Ladder Rung Walking test. The two-way *ANOVA* followed by Dunnett's test multiple comparisons test was applied intensity of HABP, number of cells enwrapped by PNNs within intact spinal cords, and for the gene expression of *has* genes. Different *post-hoc* tests for two-way ANOVA were used. Dunnett's test was used in order to test specifically the 4-MU effect and/or rehabilitation effect against a reference group (placebo without rehabilitation) in non-SCI cohorts results. Except for the two cases when the Tukey post hoc test was used for the PCR evaluation due to the reference of individual gene expression values to the untreated control without rehabilitation as well as for Maximum Speed test. Tukey test compares all possible pairs of means. For SCI cohort results, Sidak's multiple comparisons recommended for pairwise group comparisons were used. The total amount of GAGs was assessed by using the one-way *ANOVA* test followed by Dunnett's test multiple comparisons test. All the presented data in graphs were expressed as arithmetical means, with the standard error of the mean included. Significance as determined as followings: ns-not significant, $^{*}p < 0.05$ $^{**}p < 0.01$ $^{***}p < 0.001$ and $^{****}p < 0.0001$. Data were not assessed for normality. No test for outliers was conducted.

Data availability
The datasets used and/or analysed during the current study available from the corresponding author on reasonable request.

Received: 16 July 2023; Accepted: 2 November 2023
Published online: 06 November 2023

References
1. Keough, M. B. *et al.* An inhibitor of chondroitin sulfate proteoglycan synthesis promotes central nervous system remyelination. *Nat. Commun.* **7**, 11312 (2016).
2. Pinchi, E. *et al.* Acute spinal cord injury: A systematic review investigating miRNA families involved. *Int. J. Mol. Sci.* **20**, E1841 (2019).
3. Oyinbo, C. A. Secondary injury mechanisms in traumatic spinal cord injury: A nugget of this multiply cascade. *Acta Neurobiol. Exp. (Wars)* **71**, 281–299 (2011).
4. Kaplan, A., Ong Tone, S. & Fournier, A. E. Extrinsic and intrinsic regulation of axon regeneration at a crossroads. *Front. Mol. Neurosci.* **8**, 27 (2015).
5. Vogelaar, C. F. Extrinsic and intrinsic mechanisms of axon regeneration: The need for spinal cord injury treatment strategies to address both. *Neural Regen Res.* **11**, 572–574 (2016).
6. Nagappan, P. G., Chen, H. & Wang, D.-Y. Neuroregeneration and plasticity: A review of the physiological mechanisms for achieving functional recovery postinjury. *Mil. Med. Res.* **7**, 30 (2020).
7. Carulli, D. & Verhaagen, J. An extracellular perspective on CNS maturation: Perineuronal nets and the control of plasticity. *Int. J. Mol. Sci.* **22**, 2434 (2021).
8. van 't Spijker, H. M. & Kwok, J. C. F. A sweet talk: The molecular systems of perineuronal nets in controlling neuronal communication. *Front. Integr. Neurosci.* **11**, 33 (2017).
9. Pizzorusso, T. *et al.* Reactivation of ocular dominance plasticity in the adult visual cortex. *Science* **298**, 1248–1251 (2002).
10. Carulli, D. *et al.* Animals lacking link protein have attenuated perineuronal nets and persistent plasticity. *Brain* **133**, 2331–2347 (2010).
11. Tsien, R. Y. Very long-term memories may be stored in the pattern of holes in the perineuronal net. *Proc. Natl. Acad. Sci. U S A* **110**, 12456–12461 (2013).

12. Takahashi-IWANAGA, H., Murakami, T. & Abe, K. Three-dimensional microanatomy of perineuronal proteoglycan nets enveloping motor neurons in the rat spinal cord. *J. Neurocytol.* **27**, 817–827 (1998).
13. Vitellaro-Zuccarello, L., Bosisio, P., Mazzetti, S., Monti, C. & De Biasi, S. Differential expression of several molecules of the extracellular matrix in functionally and developmentally distinct regions of rat spinal cord. *Cell Tissue Res.* **327**, 433–447 (2007).
14. Galtrey, C. M., Kwok, J. C. F., Carulli, D., Rhodes, K. E. & Fawcett, J. W. Distribution and synthesis of extracellular matrix proteoglycans, hyaluronan, link proteins and tenascin-R in the rat spinal cord. *Eur. J. Neurosci.* **27**, 1373–1390 (2008).
15. Stifani, N. Motor neurons and the generation of spinal motor neuron diversity. *Front. Cell Neurosci.* **8**, 293 (2014).
16. Giamanco, K. A., Morawski, M. & Matthews, R. T. Perineuronal net formation and structure in aggrecan knockout mice. *Neuroscience* **170**, 1314–1327 (2010).
17. Irvine, S. F. & Kwok, J. C. F. Perineuronal nets in spinal motoneurones: Chondroitin sulphate proteoglycan around alpha motoneurones. *Int. J. Mol. Sci.* **19**, E1172 (2018).
18. Sorg, B. A. *et al.* Casting a wide net: Role of perineuronal nets in neural plasticity. *J. Neurosci.* **36**, 11459–11468 (2016).
19. Bradbury, E. J. *et al.* Chondroitinase ABC promotes functional recovery after spinal cord injury. *Nature* **416**, 636–640 (2002).
20. García-Alías, G., Barkhuysen, S., Buckle, M. & Fawcett, J. W. Chondroitinase ABC treatment opens a window of opportunity for task-specific rehabilitation. *Nat. Neurosci.* **12**, 1145–1151 (2009).
21. Smith, C. C. *et al.* Differential regulation of perineuronal nets in the brain and spinal cord with exercise training. *Brain Res. Bull.* **111**, 20–26 (2015).
22. Al'joboori, Y. D., Edgerton, V. R. & Ichiyama, R. M. Effects of rehabilitation on perineural nets and synaptic plasticity following spinal cord transection. *Brain Sci.* **10**, E824 (2020).
23. Stephenson, E. L. *et al.* Targeting the chondroitin sulfate proteoglycans: Evaluating fluorinated glucosamines and xylosides in screens pertinent to multiple sclerosis. *ACS Cent. Sci.* **5**, 1223–1234 (2019).
24. Dubisova, J. *et al.* Oral treatment of 4-methylumbelliferone reduced perineuronal nets and improved recognition memory in mice. *Brain Res. Bull.* **181**, 144–156 (2022).
25. Nagy, N. *et al.* 4-methylumbelliferone treatment and hyaluronan inhibition as a therapeutic strategy in inflammation, autoimmunity, and cancer. *Front. Immunol.* **6**, 123 (2015).
26. Nagy, N. *et al.* 4-Methylumbelliferyl glucuronide contributes to hyaluronan synthesis inhibition. *J. Biol. Chem.* **294**, 7864–7877 (2019).
27. Galgoczi, E. *et al.* Characteristics of hyaluronan synthesis inhibition by 4-methylumbelliferone in orbital fibroblasts. *Invest. Ophthalmol. Vis. Sci.* **61**, 27 (2020).
28. Kakizaki, I. *et al.* A novel mechanism for the inhibition of hyaluronan biosynthesis by 4-methylumbelliferone. *J. Biol. Chem.* **279**, 33281–33289 (2004).
29. Kultti, A. *et al.* 4-Methylumbelliferone inhibits hyaluronan synthesis by depletion of cellular UDP-glucuronic acid and downregulation of hyaluronan synthase 2 and 3. *Exp. Cell Res.* **315**, 1914–1923 (2009).
30. Štěpánková, K. *et al.* 4-Methylumbeliferone treatment at a dose of 1.2 g/kg/day is safe for long-term usage in rats. *Int. J. Mol. Sci.* **24**, 3799 (2023).
31. Kwok, J. C. F., Foscarin, S. & Fawcett, J. W. Perineuronal Nets: A Special Structure in the Central Nervous System Extracellular Matrix. in *Extracellular Matrix* (eds. Leach, J. B. & Powell, E. M.) 23–32 (Springer, 2015). https://doi.org/10.1007/978-1-4939-2083-9_3.
32. Reichelt, A. C., Hare, D. J., Bussey, T. J. & Saksida, L. M. Perineuronal nets: Plasticity, protection, and therapeutic potential. *Trends Neurosci.* **42**, 458–470 (2019).
33. Testa, D., Prochiantz, A. & Di Nardo, A. A. Perineuronal nets in brain physiology and disease. *Semin. Cell Dev. Biol.* **89**, 125–135 (2019).
34. Asher, R., Perides, G., Vanderhaeghen, J. J. & Bignami, A. Extracellular matrix of central nervous system white matter: Demonstration of an hyaluronate-protein complex. *J. Neurosci. Res.* **28**, 410–421 (1991).
35. Struve, J. *et al.* Disruption of the hyaluronan-based extracellular matrix in spinal cord promotes astrocyte proliferation. *Glia* **52**, 16–24 (2005).
36. Back, S. A. *et al.* Hyaluronan accumulates in demyelinated lesions and inhibits oligodendrocyte progenitor maturation. *Nat. Med.* **11**, 966–972 (2005).
37. Kuipers, H. F. *et al.* Hyaluronan synthesis is necessary for autoreactive T-cell trafficking, activation, and Th1 polarization. *Proc. Natl. Acad. Sci. U S A* **113**, 1339–1344 (2016).
38. Deepa, S. S., Yamada, S., Fukui, S. & Sugahara, K. Structural determination of novel sulfated octasaccharides isolated from chondroitin sulfate of shark cartilage and their application for characterizing monoclonal antibody epitopes. *Glycobiology* **17**, 631–645 (2007).
39. Burnside, E. R. & Bradbury, E. J. Review: Manipulating the extracellular matrix and its role in brain and spinal cord plasticity and repair. *Neuropathol. Appl. Neurobiol.* **40**, 26–59 (2014).
40. Wang, D., Ichiyama, R. M., Zhao, R., Andrews, M. R. & Fawcett, J. W. Chondroitinase combined with rehabilitation promotes recovery of forelimb function in rats with chronic spinal cord injury. *J. Neurosci.* **31**, 9332–9344 (2011).
41. Nori, S. *et al.* Human oligodendrogenic neural progenitor cells delivered with chondroitinase ABC facilitate functional repair of chronic spinal cord injury. *Stem Cell Rep.* **11**, 1433–1448 (2018).
42. Weigel, P. H. Hyaluronan synthase: The mechanism of initiation at the reducing end and a pendulum model for polysaccharide translocation to the cell exterior. *Int. J. Cell Biol.* **2015**, 367579 (2015).
43. Basso, D. M. Neuroanatomical substrates of functional recovery after experimental spinal cord injury: Implications of basic science research for human spinal cord injury. *Phys. Ther.* **80**, 808–817 (2000).
44. Kjell, J. & Olson, L. Rat models of spinal cord injury: From pathology to potential therapies. *Dis. Model Mech.* **9**, 1125–1137 (2016).
45. Stichel, C. C. & Müller, H. W. Extensive and long-lasting changes of glial cells following transection of the postcommissural fornix in the adult rat. *Glia* **10**, 89–100 (1994).
46. Hu, R. *et al.* Glial scar and neuroregeneration: histological, functional, and magnetic resonance imaging analysis in chronic spinal cord injury. *J. Neurosurg. Spine* **13**, 169–180 (2010).
47. Oudega, M., Bradbury, E. J. & Ramer, M. S. Combination therapies. *Handb. Clin. Neurol.* **109**, 617–636 (2012).
48. Fawcett, J. W. & Curt, A. Damage control in the nervous system: Rehabilitation in a plastic environment. *Nat. Med.* **15**, 735–736 (2009).
49. Kanagal, S. G. & Muir, G. D. Task-dependent compensation after pyramidal tract and dorsolateral spinal lesions in rats. *Exp. Neurol.* **216**, 193–206 (2009).
50. Jacobs, B. L., Martín-Cora, F. J. & Fornal, C. A. Activity of medullary serotonergic neurons in freely moving animals. *Brain Res. Rev.* **40**, 45–52 (2002).
51. Jordan, L. M., Liu, J., Hedlund, P. B., Akay, T. & Pearson, K. G. Descending command systems for the initiation of locomotion in mammals. *Brain Res. Rev.* **57**, 183–191 (2008).
52. Murray, K. C. *et al.* Recovery of motoneuron and locomotor function after spinal cord injury depends on constitutive activity in 5-HT2C receptors. *Nat. Med.* **16**, 694–700 (2010).
53. Schmidt, B. J. & Jordan, L. M. The role of serotonin in reflex modulation and locomotor rhythm production in the mammalian spinal cord. *Brain Res. Bull.* **53**, 689–710 (2000).

54. Hayashi, Y. *et al.* 5-HT precursor loading, but not 5-HT receptor agonists, increases motor function after spinal cord contusion in adult rats. *Exp. Neurol.* **221**, 68–78 (2010).
55. Harvey, P. J., Li, X., Li, Y. & Bennett, D. J. 5-HT2 receptor activation facilitates a persistent sodium current and repetitive firing in spinal motoneurons of rats with and without chronic spinal cord injury. *J. Neurophysiol.* **96**, 1158–1170 (2006).
56. Chen, B. *et al.* Reactivation of dormant relay pathways in injured spinal cord by KCC2 manipulations. *Cell* **174**, 1599 (2018).
57. Barzilay, R. *et al.* CD44 deficiency is associated with increased susceptibility to stress-induced anxiety-like behavior in mice. *J. Mol. Neurosci.* **60**, 548–558 (2016).
58. Perrier, J.-F. & Delgado-Lezama, R. Synaptic release of serotonin induced by stimulation of the raphe nucleus promotes plateau potentials in spinal motoneurons of the adult turtle. *J. Neurosci.* **25**, 7993–7999 (2005).
59. Perrier, J.-F. & Hounsgaard, J. 5-HT2 receptors promote plateau potentials in turtle spinal motoneurons by facilitating an L-type calcium current. *J. Neurophysiol.* **89**, 954–959 (2003).
60. Harvey, P. J., Li, Y., Li, X. & Bennett, D. J. Persistent sodium currents and repetitive firing in motoneurons of the sacrocaudal spinal cord of adult rats. *J. Neurophysiol.* **96**, 1141–1157 (2006).
61. Bennett, D. J. *et al.* Spasticity in rats with sacral spinal cord injury. *J. Neurotrauma* **16**, 69–84 (1999).
62. Bennett, D. J., Sanelli, L., Cooke, C. L., Harvey, P. J. & Gorassini, M. A. Spastic long-lasting reflexes in the awake rat after sacral spinal cord injury. *J. Neurophysiol.* **91**, 2247–2258 (2004).
63. Button, D. C. *et al.* Does elimination of afferent input modify the changes in rat motoneurone properties that occur following chronic spinal cord transection?. *J. Physiol.* **586**, 529–544 (2008).
64. Barbeau, H., Fung, J., Leroux, A. & Ladouceur, M. A review of the adaptability and recovery of locomotion after spinal cord injury. *Prog. Brain Res.* **137**, 9–25 (2002).
65. Wirz, M. *et al.* Effectiveness of automated locomotor training in patients with chronic incomplete spinal cord injury: A multicenter trial. *Arch. Phys. Med. Rehabil.* **86**, 672–680 (2005).
66. Ballermann, M. & Fouad, K. Spontaneous locomotor recovery in spinal cord injured rats is accompanied by anatomical plasticity of reticulospinal fibers. *Eur. J. Neurosci.* **23**, 1988–1996 (2006).
67. Bareyre, F. M. *et al.* The injured spinal cord spontaneously forms a new intraspinal circuit in adult rats. *Nat. Neurosci.* **7**, 269–277 (2004).
68. Courtine, G. *et al.* Recovery of supraspinal control of stepping via indirect propriospinal relay connections after spinal cord injury. *Nat. Med.* **14**, 69–74 (2008).
69. Vavrek, R., Girgis, J., Tetzlaff, W., Hiebert, G. W. & Fouad, K. BDNF promotes connections of corticospinal neurons onto spared descending interneurons in spinal cord injured rats. *Brain* **129**, 1534–1545 (2006).
70. Hawthorne, A. L. *et al.* The unusual response of serotonergic neurons after CNS Injury: Lack of axonal dieback and enhanced sprouting within the inhibitory environment of the glial scar. *J. Neurosci.* **31**, 5605–5616 (2011).
71. Skene, J. H. & Willard, M. Characteristics of growth-associated polypeptides in regenerating toad retinal ganglion cell axons. *J. Neurosci.* **1**, 419–426 (1981).
72. Jacobson, R. D., Virág, I. & Skene, J. H. A protein associated with axon growth, GAP-43, is widely distributed and developmentally regulated in rat CNS. *J. Neurosci.* **6**, 1843–1855 (1986).
73. Donovan, S. L., Mamounas, L. A., Andrews, A. M., Blue, M. E. & McCasland, J. S. GAP-43 is critical for normal development of the serotonergic innervation in forebrain. *J. Neurosci.* **22**, 3543–3552 (2002).
74. Bendotti, C., Servadio, A. & Samanin, R. Distribution of GAP-43 mRNA in the brain stem of adult rats as evidenced by in situ hybridization: Localization within monoaminergic neurons. *J. Neurosci.* **11**, 600–607 (1991).
75. Vigetti, D. *et al.* The effects of 4-methylumbelliferone on hyaluronan synthesis, MMP2 activity, proliferation, and motility of human aortic smooth muscle cells. *Glycobiology* **19**, 537–546 (2009).
76. Abate, A. *et al.* Hymecromone in the treatment of motor disorders of the bile ducts: A multicenter, double-blind, placebo-controlled clinical study. *Drugs Exp. Clin. Res.* **27**, 223–231 (2001).
77. Camarri, E. & Marchettini, G. Hymecromone in the treatment of symptoms following surgery of the bile ducts. *Recent. Prog. Med.* **79**, 198–202 (1988).
78. Krawzak, H. W., Heistermann, H. P., Andrejewski, K. & Hohlbach, G. Postprandial bile-duct kinetics under the influence of 4-methylumbelliferone (hymecromone). *Int. J. Clin. Pharmacol. Ther.* **33**, 569–572 (1995).
79. Quaranta, S., Rossetti, S. & Camarri, E. Double-blind clinical study on hymecromone and placebo in motor disorders of the bile ducts after cholecystectomy. *Clin. Ter* **108**, 513–517 (1984).
80. Trabucchi, E. *et al.* Controlled study of the effects of tiropramide on biliary dyskinesia. *Pharmatherapeutica* **4**, 541–550 (1986).
81. Walter, P. & Seidel, W. Studies on the effect of 4-methyl-umbelliferon (Hymecromone) in patients following surgical revision of the biliary pathways. *Chirurg* **50**, 436–440 (1979).
82. Hoffmann, R. M., Schwarz, G., Pohl, C., Ziegenhagen, D. J. & Kruis, W. Bile acid-independent effect of hymecromone on bile secretion and common bile duct motility. *Dtsch Med. Wochenschr* **130**, 1938–1943 (2005).
83. Sengupta, P. The laboratory rat: Relating its age with human's. *Int. J. Prev. Med.* **4**, 624–630 (2013).
84. Livak, K. J. & Schmittgen, T. D. Analysis of relative gene expression data using real-time quantitative PCR and the 2(-Delta Delta C(T)) Method. *Methods* **25**, 402–408 (2001).
85. Basso, D. M., Beattie, M. S. & Bresnahan, J. C. A sensitive and reliable locomotor rating scale for open field testing in rats. *J. Neurotrauma* **12**, 1–21 (1995).
86. Metz, G. A. & Whishaw, I. Q. The ladder rung walking task: A scoring system and its practical application. *J. Vis. Exp.* **1204**, 1. https://doi.org/10.3791/1204 (2009).

Acknowledgements

Supported by: Center of Reconstruction Neuroscience—NEURORECON CZ.02.1.01/0.0/0.0/15_003/0000419 (to LMU, PV and JCFK) and Czech Science Agency 19-10365S (to PV and JCFK). Wings for Life (WFL-UK-008-15) and Medical Research Council UK (Confidence in concept MC-PC-16050 and Project grant MR/S011110/1) to JCFK. *Microscopy was done at the Microscopy Service Centre of the Institute of Experimental Medicine CAS supported by the MEYS CR (LM2023050 Czech-Bioimaging)* and the BioImaging facility at the University of Leeds (Wellcome Trust, WT104818MA).

Author contributions

K.S., M.C., S.K., L.M.U., P.J., J.C.F.K. conceived and/or designed the study. S.K., L.M.U., P.J. and J.C.F.K. obtained funding. K.S., M.C., Z.S., N.M.V. and L.M.U. performed the experiments. K.S., M.C., S.K., L.M.U., P.J. and J.C.F.K. analysed and interpreted data, all authors were involved in the writing and revising the manuscript.

Competing interests

Kwok has a patent 'Treatment of Conditions of the Nervous System' (PCT/EP2020/079979) issued. Remaining author has no competing to declare.

Additional information

Correspondence and requests for materials should be addressed to K.Š., L.M.U., P.J. or J.C.F.K.

Reprints and permissions information is available at www.nature.com/reprints.

Publisher's note Springer Nature remains neutral with regard to jurisdictional claims in published maps and institutional affiliations.